原　著

Pyothorax-associated Lymphoma : Loss of Epstein-Barr Virus Nuclear Antigen-3B Protein Expression as a Result of Mismatch Repair Phenotypes

Tetsuya TAKAKUWA

Abstracts : Pyothorax-associated lymphoma (PAL) is an EBV-associated lymphoma, which develops in the pleural cavity of immunocompetent patients with an over-20-year history of pyothorax.　PAL tumor cells taken from a 72-year-old man revealed having mismatch repair (MMR) phenotype and expression of all Epstein-Barr virus latent genes except EBNA-3B.　EBNA-3B gene in the derived cell line had frameshift mutation in mononucleotide repeats, indicating that EBNA-3B was the target for the MMR phenotype. Because EBNA-3B works as target antigens for host cytotoxic T-lymphocyte (CTL) responses via two HLA-A11-restricted epitopes, loss of EBNA-3B expression may contribute for PAL cells to escape from host immune surveillance in the present case.

Key words : Pyothorax-associated lymphoma, Epstein-Barr virus, EBNA-3B, Mismatch repair phenotypes

Introduction

Malignant lymphoma frequently develops in the pleural cavity of patients with over 20-year history of pyothorax[1]. This tumor stand as a distinct clinicopathologic entity, thus the term pyothorax-associated lymphoma (PAL) has been proposed for this type of tumor[2].　PAL is now listed as a distinct disease entity in the recent World Health Organization Classification of tumors[3].　PAL is non-Hodgkin lymphoma, mostly diffuse large B-cell lymphoma (DLBCL), which is strongly associated with Epstein-Barr virus (EBV) infection.

Previous study on a relatively small number of PAL cases reported the Latency (Lat) III pattern of EBV infection at protein level, i.e. the tumor cells express all 9 latent genes[4]. Whereas, we recently demonstrated that the EBV latency pattern in PAL was various among cases[5].　Latent infection antigens of EBV, including EBV nuclear antigens (EBNAs) and latent membrane proteins, are expressed in latently infected and immortalized B cells but they work as target antigens for host cytotoxic T-lymphocyte (CTL) responses in a HLA class I-restricted manner[6,7].　Among these latent antigens, the immunodominant CTL epitopes in EBNA-3B (EBNA-3B 399-408 and EBNA-3B 416-424) are well characterized.　The major cytolytic activity of the host CTL is induced via two HLA-A11-restricted epitopes in the viral EBNA-3B antigen[6,7].

Usually, there are no clinical findings suggesting the presence of immune dysfunction in patients with PAL[1,2]. Therefore some mechanism for PAL cells to escape from host immune surveillance must be present.　Production of immunosuppressive cytokine IL-10 by PAL cells, decreased of expression of HLA class I molecules in PAL cells, or mutation of CTL-epitope in EBNA3B might be involved in the escape of PAL cells from CTL[8-10].

We have established several cell lines from PAL tissues[11]; among them one line (OPL-3) with Lat III pattern of latent gene expression did not express EBNA-3B protein. Sequencing analysis revealed frameshift mutations in mononucleotide repeats within EBNA-3B gene, which generates premature stop codon, thus abolish EBNA-3B protein expression.　In addition to reduction of HLA class 1 molecules, loss of the EBNA-3B expression may contribute to PAL cells to escape from host immune surveillance.　The host tumor cells were mismatch repair (MMR) phenotype, which may cause in mutations of EBNA-3B genes.

Case report

A 72-year-old man was admitted to National Kinki-Chuou Hospital with left chest pain.　He had suffered from pulmonary tuberculosis in the left lung and received an artificial pneumothorax when he was 22 years old. Computed tomographic (CT) scan on admission of this time revealed the masses in the left pleural cavity and diaphragm,
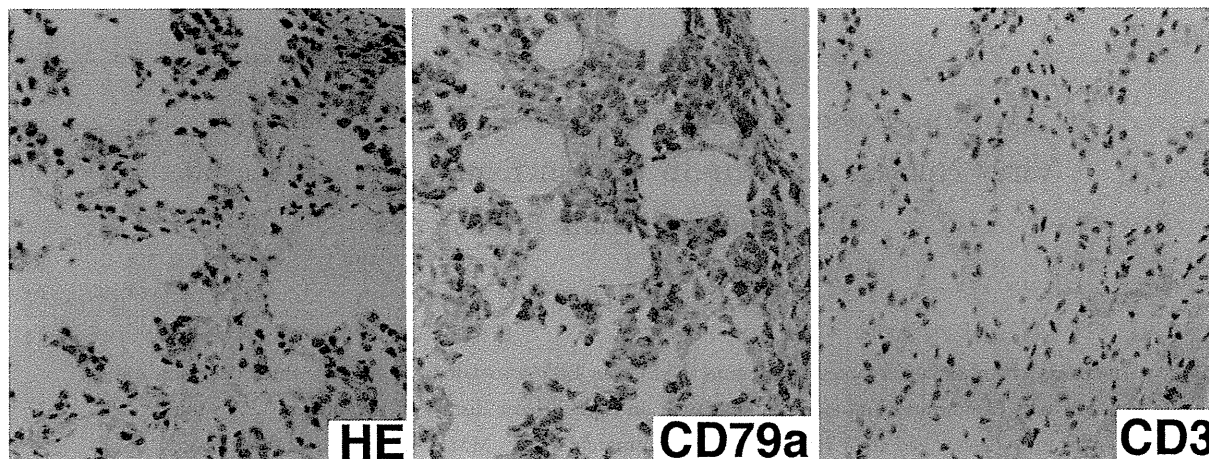
Fig. 1 Aspiration biopsy from the pleural cavity revealed a monomorphous proliferation of large lymphoid cells in the collagens and fat tissues (HE).　Immunohistochemistry revealed that these cells were positive for CD79a and negative for CD3, thus diagnosed as diffuse large lymphoma of B-cell type.　Few intermingling small lymphocytes were observed.

which were affected by pyothorax.　Aspiration biopsy from the pleura revealed monomorphic proliferation of large lymphoid cells in the collagens and fat tissues (Fig. 1). Immunohistochemistry revealed that most proliferating cells were positive for CD20 and CD79a, and negative for CD3, thus diagnosed as diffuse large lymphoma of B-cell type.

Fig. 2 Flow-cytometric analyses for expression of HLA class I antigens in PAL cell lines OPL-3 and EBV infected peripheral B lymphocytes (lymphoblastoid cell line ; LCL).　Cells were incubated with HLA class I monoclonal antibody (white) or with control antibodies (shaded), incubated with FITC-labeled second antibodies, and analyzed with a flow-cytometry.

As for EBV gene expression, both LMP-1 and EBNA-2 were positive in immunohistochemistry.　A cell line was established from a part of the sample with informed consent in accordance with the Declaration of Helsinki[11].　HLA-A allele of the patient was A2/A11 (data not shown).　Flow-cytometric analyses of the cell line revealed slightly reduced, but definite expression of HLA class I molecule (Fig. 2). Radiographic examination including abdominal CT, brain magnetic resonance imaging, and Gallium scintigraphy together with bone marrow biopsy revealed metastasis in the spleen.　Combined two courses of chemotherapy (cyclophosphamide, doxorubicin, vincristine, and prednisolone) and 50 Gy of radiation therapy were started, but he died of disease 30 months after admission.　Autopsy was not performed.

Materials and Methods

1.　HLA-A allotyping and flow-cytometric analysis for HLA class I

Low-resolution HLA-A locus-specific PCR typing of the patient was performed using HLA-A locus sequence-specific primers combinations in PCR amplification of genomic DNA as described previously[9].　Flow-cytometric analysis for expression of HLA class I molecule in the cell lines was done.

2.　RT-PCR analysis for detection of EBV latent gene expression

Total RNA was extracted from the samples with the TRIzol reagent (Invitrogen, Inc., Rockville, MD) according to the manufacturer's instructions.　Five μg of total RNA were reverse-transcribed by random hexamer priming using the Superscript first strand synthesis system (Invitrogen). Primer pairs were designed to distinguish different EBNA-1 promoter usage from each other, and to detect EBNA-2 and
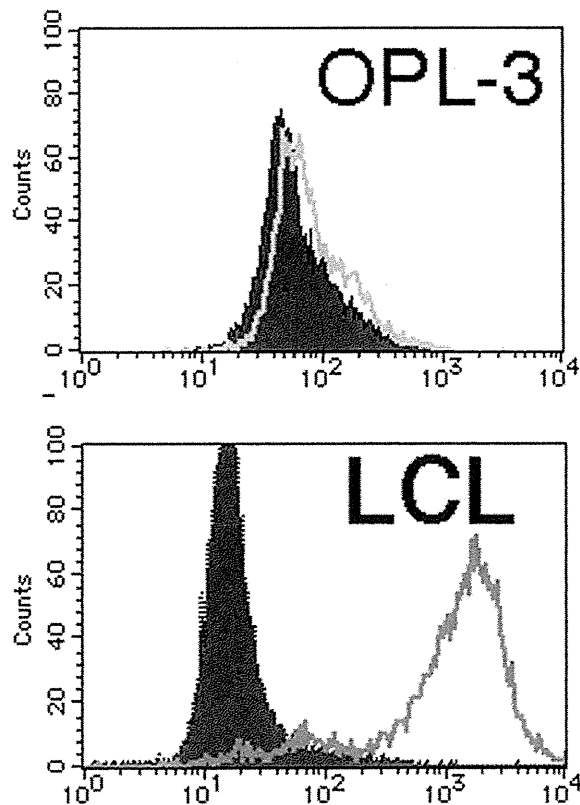
EBNA-3B transcripts as described previously[5,12].

3. Detection of mutations

Long-distance PCR was performed to amplify the whole EBNA-3B gene. After electrophoresis on 1.0% agarose gel, DNA fragments were excised and purified using the Wizard SV gel extraction kit (Promega Co., Madison, WI). The purified DNA was used as template for PCR, and the products were directly sequenced with appropriate primers.

4. Western blotting

Western blotting was carried out as described previously[13]. Briefly, whole cells were lyzed in 1 x sample buffer, separated with 10% SDS-PAGE, and then blotted to polyvinylidene difluoride membrane using a wet-blotting apparatus. Anti-LMP-1 and -EBNA-2 antibodies were purchased from DAKO (Glostrup, Denmark), and anti-EBNA-3B antibody from Exalpha Biologicals (Boston, MA). Anti-actin antibody (Sigma, St. Louis, MO) was used as control. Signals were visualized with ECL plus Chemiluminescent reagents (GE Healthcare Bio-Sciences
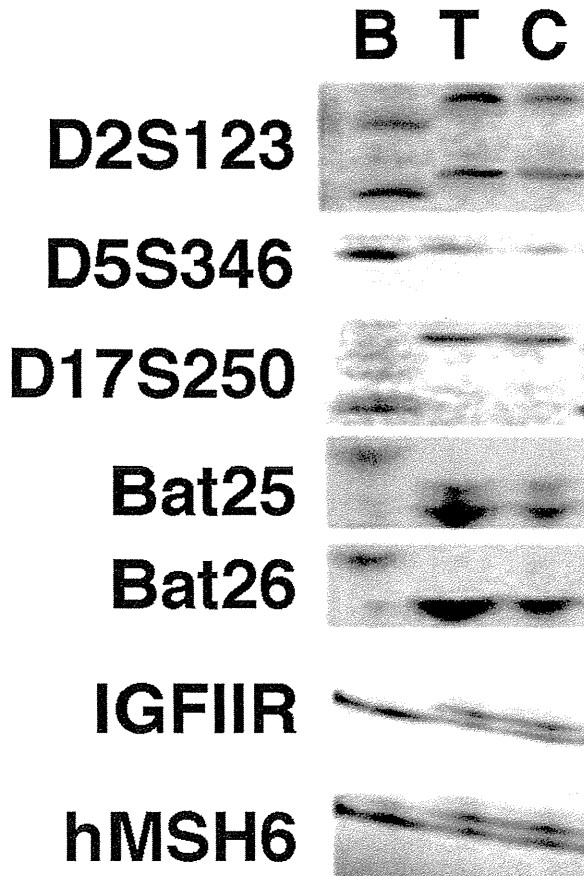

Fig. 4 Analysis of EBNA-1 promoter usage and expression of EBNA-2, and -3B transcripts in OPL-3. Products were visualized on agarose gels stained with ethidium bromide.

Corp., Piscataway, NJ).

Results

The cell line (OPL-3) established from the patient was an immunophenotype of B cell and similar to that of the original biopsy specimen (i.e. positive for CD20, CD30 and CD79a, and negative for CD3, CD4, CD5, CD7, and CD8), which were confirmed with three different subclones. Terminal repeat of fusion of EBV in lymphoma cells was monoclonal pattern. Karyotype was complex with numerous structural and numerical abnormalities. Disruption of the MMR system, as revealed by Microsatellite Instability (MSI) was found (Fig. 3)[11]. According to the International Workshop on MSI and RER phenotypes in Cancer Detection and Familial Predisposition[14], four of five microsatellite repeats were positive. MMR target genes such as *IGFIIR* and *hMSH6* were also mutated. Promoter usage of EBNA-1 was Lat III pattern in OPL-3 (Fig. 4). LMP-1, EBNA-2, and EBNA-3B were also expressed as expected. LMP-1 and EBNA-2 proteins were expressed as well, whereas, EBNA-3B protein was not detected by Western Blotting analysis (Fig. 5).

Sequencing analysis of EBNA-3B in OPL-3 and peripheral blood leukocytes from the patient was performed. Compared with EBV genome in the strain B95-8, (Gene Acc V01555.2), more than 10 polymorphisms were observed in EBNA-3B from both OPL-3 and

Fig. 3 According to the International Workshop on MSI and RER phenotypes in Cancer Detection and Familial Predisposition, five microsatellite repeats, D2S123, D5S346, D17S250, BAT25, and BAT26 were analyzed in OPL-3. MMR-target genes such as IGFIIR and hMSH6 were mutated. PCR products from established cell line (C), tumor (T) and corresponding peripheral blood leukocytes (B).
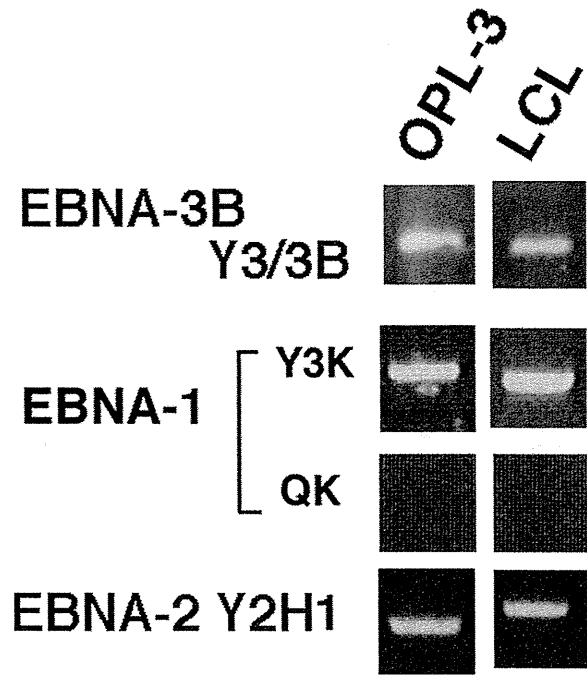
EBNA-3B

EBNA-1
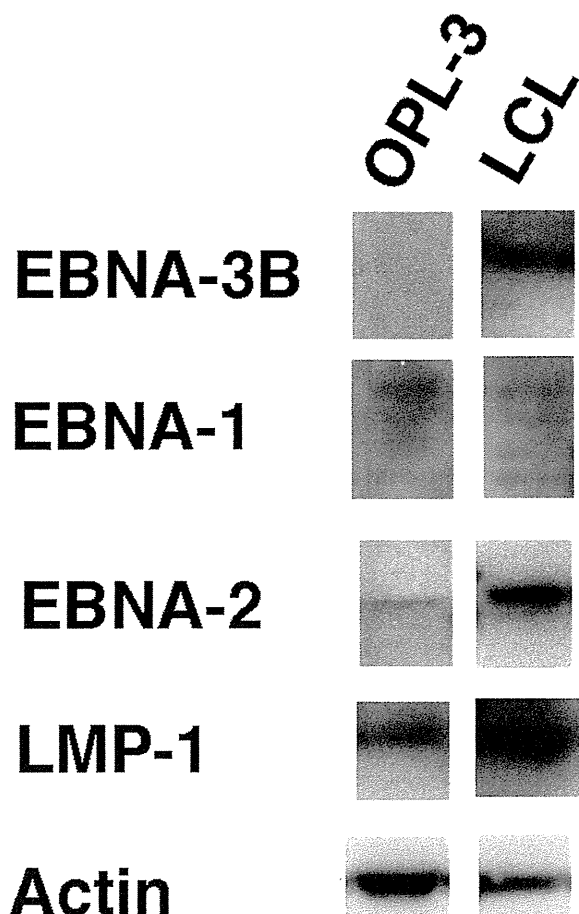
EBNA-2

LMP-1

Actin

Fig. 5 Latent gene protein expression in PAL cell lines by Western blotting. Expression of EBNA-3B was not detected in OPL-3.

peripheral blood leukocytes (data not shown). Frameshift mutation at mononucleotide tracts from nucleotide 96007 to 96013 in OPL-3, which generates premature stop codon, was observed in OPL-3 but not in the peripheral blood leukocytes (Fig. 6).

Change in mononucleotide repeat lengths was not observed in other EBV latent genes including, LMP-1 (poly C7 ; nt number 5804-5810 in B95-8), EBNA-2 (poly C8 ; nt number 48696-48703), EBNA-3A (poly C7 ; nt number 94177-94183, nt number 94697-94703), EBNA-3B (poly A7 ; nt number 95887-95893, poly G7 ; nt number 95387-95393, nt number 95999-96005, number 98075-98081), EBNA-3C (poly C7 ; nt number 100738-100744), EBNA-1 (poly G7 ; nt number 107026-107032) as well as OriP regions (poly A8 ; nt number 8339-8346, poly C8 ; nt number 9439-9446) (data not shown).

Discussion

PAL is an EBV-associated lymphoma, which develops in patients with over 20 year-history of chronic pyothorax and with no evidence of immune dysfunction[1,2]. Because most PAL expresses full range of EBV latent genes, escape mechanisms from host CTL should work in PAL[4-7]. Indeed, OPL-3 showed the Lat III pattern of EBV latent gene expression and expressed HLA-A11. However, histologic examination of biopsy sample did not reveal the
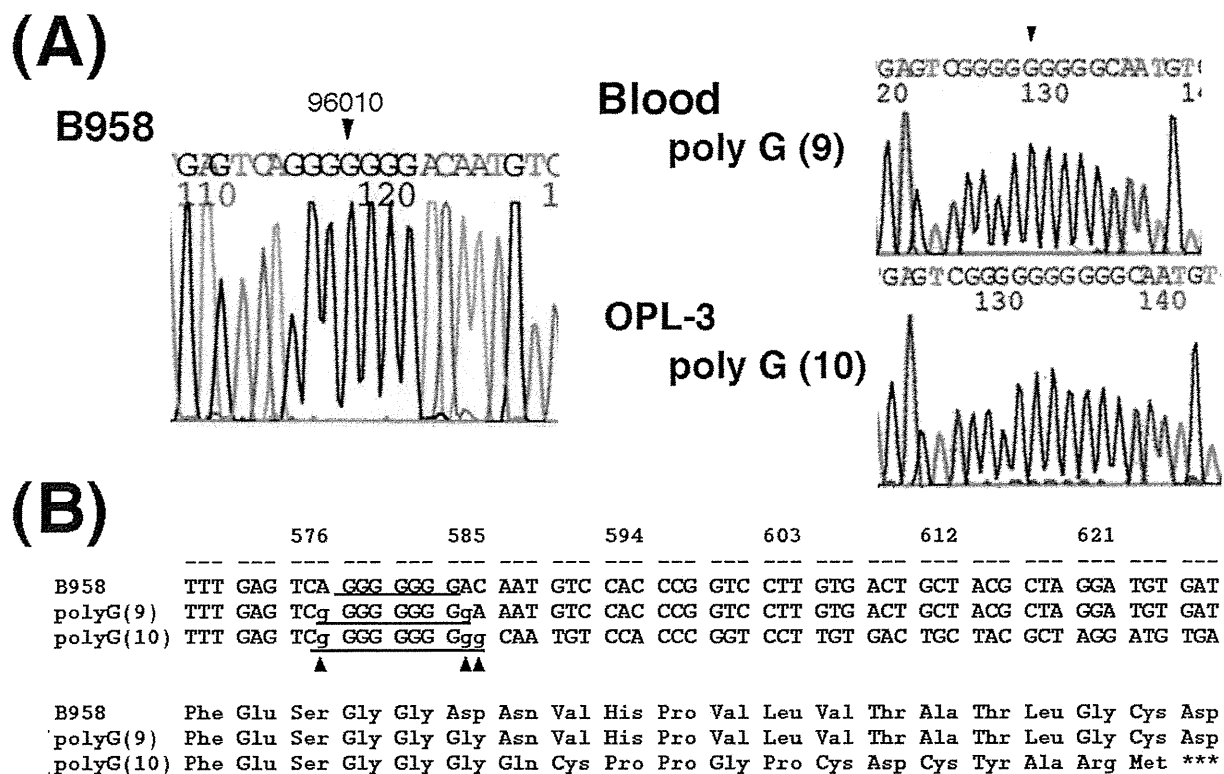
(A)

B958

Blood
poly G (9)

OPL-3
poly G (10)

(B)

		576			585			594			603			612			621		
B958	TTT	GAG	TCA	GGG	GGG	GAC	AAT	GTC	CAC	CCG	GTC	CTT	GTG	ACT	GCT	ACG	CTA	GGA	TGT	GAT
polyG(9)	TTT	GAG	TCg	GGG	GGG	GgA	AAT	GTC	CAC	CCG	GTC	CTT	GTG	ACT	GCT	ACG	CTA	GGA	TGT	GAT
polyG(10)	TTT	GAG	TCg	GGG	GGG	Ggg	CAA	TGT	CCA	CCC	GGT	CCT	TGT	GAC	TGC	TAC	GCT	AGG	ATG	TGA

B958	Phe	Glu	Ser	Gly	Gly	Asp	Asn	Val	His	Pro	Val	Leu	Val	Thr	Ala	Thr	Leu	Gly	Cys	Asp
polyG(9)	Phe	Glu	Ser	Gly	Gly	Gly	Asn	Val	His	Pro	Val	Leu	Val	Thr	Ala	Thr	Leu	Gly	Cys	Asp
polyG(10)	Phe	Glu	Ser	Gly	Gly	Gly	Gln	Cys	Pro	Pro	Gly	Pro	Cys	Asp	Cys	Tyr	Ala	Arg	Met	***

Fig. 6 Sequencing of EBNA-3B gene containing at mononucleotide tracts from nucleotide 96007 to 96013 (A) and predicted amino acid sequences in OPL-3 (B). Frameshift mutation was observed in OPL-3, which gnerate premature stop codon. No frame shift mutations were observed in peripheral blood leukocytes. B95-8 sequence was shown as comparison.

findings suggestive of CTL response against the proliferating PAL cells, i.e., infiltration of T lymphocytes.

EBNA-3B protein was not expressed in OPL-3. The sequencing analysis revealed the frameshift mutations within EBNA-3B gene, which might result in loss of the EBNA-3B protein. The mutations were insertions within mononucleotide repeats, which are frequently observed in cells with MMR phenotypes. In the previous report[11], we demonstrated that OPL-3 had MMR phenotypes and MMR-target genes such as IGFIIR and hMSH6 was mutated. Because EBV replication is synchronized with host cell division using the host replication system, the simple repeat sequences in EBV genome might also be the target in the host with MMR phenotype. EBV genome contains many mononucleotide repeats. In the present study the insertion G was observed in only EBNA-3B gene in OPL-3. Further in vitro and *in vivo* study may be necessary whether loss of EBNA-3B may be growth advantage or not.

MMR type is rare in non-Hodgkin lymphoma except for immunodeficiency-related lymphoma such as HIV infection-related lymphomas and posttransplant lymphoproliferative disorders[15]. Immunotherapy employing antigen-specific T cells for treatment of human malignancies is becoming popular. EBNA-3B epitope is one of the candidates for the virus-specific CTL therapy in fatal lymphoproliferative diseases. Gottschalk et al reported a case in which CTL therapy to fatal lymphoproliferative disease resulted in the selection of clone with EBNA-3B deletion[16]. It is possible that EBNA-3B deletion clone might be selected in such lymphomas as same mechanism as observed in the present case.

The present case suggests that not only host genome but also infected EBV genome could be targets for mutations in cells with MMR phenotype. Resultant loss of latent gene EBNA-3B expression provides an advantage for tumor growth via escape from host CTL responses. This seems to be one of the mechanisms how PAL cells avoid from CTL response. It is interesting to know whether other EBV-related lymphomas have deficiency in EBNA-3B expression.

References

1) Nakatsuka S, Yao M, Hoshida Y, Yamamoto S, Iuchi K, Aozasa K : Pyothorax-associated lymphoma : a review of 106 cases. J Clin Oncol, 2003 ; 20 : 4255-4260

2) Iuchi K, Aozasa K, Yamamoto S, et al : Non-Hodgkin's lymphoma of the pleural cavity developing from long-standing pyothorax. Summary of clinical and pathological findings in thirty-seven cases. Jpn J Clin Oncol, 1989 ; 19 : 249-257

3) Banks PM, Harris NL, Warnke RA, Gaulard Ph : Lymphomas.

In : Travis WD, Brambilla E, Mueller-Hermelink HK, Harris CC, eds. World Health Organization Classification of Tumors : Pathology and Genetics of tumors of the Lung, Pleura, Thymus and Heart. Lyon : IARC Press, 2004 : 137-140

4) Fukayama M, Ibuka T, Hayashi Y, Ooba T, Koike M, Mizutani S : Epstein-Barr virus in pyothorax-associated pleural lymphoma. Am J Pathol, 1993 ; 143 : 1044-1049

5) Takakuwa T, Ham MF, Luo WJ, Nakatsuka S, Daibata M, Aozasa K : Loss of expression of Epstein-Barr virus nuclear antigen-2 correlates with a poor prognosis in cases of pyothorax-associated lymphoma. Int J Cancer, 2006 ; 118 : 2782-2789

6) de Campos-Lima PO, Levitsky V, Brooks J, et al : T cell responses and virus evolution : loss of HLA A11-restricted CTL epitopes in Epstein-Barr virus isolates from highly A11-positive populations by selective mutation of anchor residues. J Exp Med, 1994 ; 179 : 1297-1305

7) Rickinson AB, Moss DJ : Human cytotoxic T lymphocyte responses to Epstein-Barr virus infection. Annu Rev Immunol, 1997 ; 15 : 405-431

8) Kanno H, Nakatsuka S, Iuchi K, Aozasa K : Sequences of cytotoxic T-lymphocyte epitopes in the Epstein-Barr virus (EBV) nuclear antigen-3B gene in a Japanese population with or without EBV-positive lymphoid malignancies. Int J Cancer, 2000 ; 88 : 626-632

9) Kanno H, Ohsawa M, Hashimoto M, Iuchi K, Nakajima Y, Aozasa K : HLA-A alleles of patients with pyothorax-associated lymphoma : anti-Epstein-Barr virus (EBV) host immune responses during the development of EBV latent antigen-positive lymphomas. Int J Cancer, 1999 ; 82 :630-634

10) Kanno H, Naka N, Yasunaga Y, et al : Production of the immunosuppressive cytokine interleukin-10 by Epstein-Barr virus expressing pyothorax-associated lymphoma : possible role in the development of overt lymphoma in immunocompetent hosts. Am J Pathol, 1997 ; 150 : 349-357

11) Takakuwa T, Luo WJ, Ham MF, Mizuki M, Iuchi K, Aozasa K : Establishment and characterization of unique cell lines derived from pyothorax-associated lymphoma which develops in long-standing pyothorax and is strongly associated with Epstein-Barr virus infection. Cancer Sci, 2003 ; 94 : 858-863

12) Oudejans JJ, van den Brule AJ, Jiwa NM, et al : BHRF1, the Epstein-Barr virus (EBV) homologue of the BCL-2 protooncogene, is transcribed in EBV-associated B-cell lymphomas and in reactive lymphocytes. Blood, 1995 ; 86: 1893-1902

13) Liu A, Takakuwa T, Fujita S, et al : Alterations of DNA damage-response genes ATM and ATR in pyothorax-associated lymphoma. Lab Invest, 2005 ; 85 : 436-446

14) Boland CR, Thibodeau SN, Hamilton SR, et al : A National Cancer Institute Workshop on Microsatellite Instability for cancer detection and familial predisposition : development of international criteria for the determination of microsatellite instability in colorectal cancer. Cancer Res, 1998 ; 58 : 5248-5257

15) Duval A, Raphael M, Brennetot C, et al : The mutator pathway is a feature of immunodeficiency-related lymphomas. Proc Natl Acad Sci USA, 2004 ; 101 : 5002-5007

16) Gottschalk S, Ng CY, Perez M, et al: An Epstein-Barr virus deletion mutant associated with fatal lymphoproliferative disease unresponsive to therapy with virus-specific CTLs. Blood, 2001 ; 97 : 835-843

ミスマッチ修復異常によって EBNA-3B 蛋白の発現消失を来したと考えられる膿胸関連リンパ腫の1例

高　桑　徹　也

要　　　約

膿胸関連リンパ腫 (PAL) は Epstein-Barr ウイルス (EBV) 関連リンパ腫の一つで，免疫能低下などのみられない慢性膿胸の患者において，20年以上の慢性炎症を経て胸腔に発症する。72歳の男性症例から採取された同リンパ腫において EBV の潜伏遺伝子の発現は EBNA-3B 遺伝子を除いて発現が認められた。EBNA-3B 蛋白は宿主の CTL 応答の標的として働くので，その発現消失は，免疫監視機構を回避し腫瘍増殖に有利に働いた可能性がある。EBNA-3B 遺伝子の塩基配列を検討すると単塩基重複配列部分に塩基の欠失がみられた。このような欠失はミスマッチ修復異常 (MMR type) により生じることが知られ，同腫瘍細胞も MMR type であった。宿主の MMR type が感染した EBV ゲノム変異に影響を及ぼした点は大変興味深い。

Efficient generation of transgene-free human induced pluripotent stem cells (iPSCs) by temperature-sensitive Sendai virus vectors

Hiroshi Ban[a,1], Naoki Nishishita[b,c,1], Noemi Fusaki[a,d,2], Toshiaki Tabata[a], Koichi Saeki[a], Masayuki Shikamura[c], Nozomi Takada[c], Makoto Inoue[a], Mamoru Hasegawa[a], Shin Kawamata[b,c,2], and Shin-Ichi Nishikawa[b,c]

[a]DNAVEC Corporation, Tsukuba, Ibaraki 300-2611, Japan; [b]RIKEN Center for Developmental Biology, Kobe, Hyogo 650-0047, Japan; [c]Foundation for Biomedical Research and Innovation, Kobe, Hyogo 650-0043, Japan; and [d]Precursory Research for Embryonic Science and Technology, Japan Science and Technology Agency, Kawaguchi, Saitama 332-0012, Japan

After the first report of induced pluripotent stem cells (iPSCs), considerable efforts have been made to develop more efficient methods for generating iPSCs without foreign gene insertions. Here we show that Sendai virus vector, an RNA virus vector that carries no risk of integrating into the host genome, is a practical solution for the efficient generation of safer iPSCs. We improved the Sendai virus vectors by introducing temperature-sensitive mutations so that the vectors could be easily removed at non-permissive temperatures. Using these vectors enabled the efficient production of viral/factor-free iPSCs from both human fibroblasts and CD34+ cord blood cells. Temperature-shift treatment was more effective in eliminating remaining viral vector-related genes. The resulting iPSCs expressed human embryonic stem cell markers and exhibited pluripotency. We suggest that generation of transgene-free iPSCs from cord blood cells should be an important step in providing allogeneic iPSC-derived therapy in the future.

regenerative medicine | nonintegrating RNA vector

S afer and more efficient reprogramming methods have been explored since the first report of the generation of human induced pluripotent stem cells (iPSCs) (1, 2). Toward this end, several techniques have been used for obtaining integration and/or transgene-free iPSCs, including the use of plasmids (3, 4), the Cre/loxP system (5, 6), adenoviruses (7), piggyBac (8, 9), minicircle vector (10), and proteins (11, 12). However, these methods suffer from low efficiency, require repetitive induction, and/or produce insufficient excision of integrated vectors. Synthetic modified mRNA may solve the problem, but the reagents must be added every day (13). Thus, more efficient and simple methods are needed to generate human iPSCs with no noise of integration or remaining factors for both clinical applications and basic studies.

An alternative technology involves the use of Sendai virus (SeV) vectors. SeV, a member of the *Paramyxovirdae* family, is an enveloped virus with a single-stranded, negative-sense, non-segmented RNA genome of ~15 kb (14). Importantly, recombinant SeV vectors replicate only in the cytoplasm of infected cells and do not go through a DNA phase or integrate into the host genome (15). SeV vectors have proven to be efficient for the introduction of foreign genes in a wide spectrum of host cell species and tissues, and SeV vectors have been studied for applying to clinical studies of gene therapy for cystic fibrosis, critical limb ischemia, vaccines for AIDS, and other areas (reviewed in ref. 16). We previously reported that the SeV vectors efficiently generate human iPSCs from human fibroblasts (17) and human blood cells (18). However, to apply SeV vector technology to the generation of safer iPSCs, the issue of the sustained cytoplasmic replication of viral vectors after the iPSCs have been established had to be overcome, even though viral vectors are slowly diluted during the robust cell division of iPSCs and SeV vector–positive cells can be removed using an anti–SeV-HN antibody (17). In

other words, a more efficient shutdown of viral replication is needed to generate human iPSCs. We considered the use of temperature-sensitive (TS) SeV vectors the likeliest best solution.

Here we show that by introducing point mutations in the polymerase-related genes, we obtained new TS vectors and efficiently generated viral/factor-free human iPSCs from fibroblasts using these vectors by two strategies, (*i*) replacing the MYC vector only and (*ii*) replacing all reprogramming vectors to the TS vectors. We also applied this method to CD34+ cord blood (CB) cells because SeV vector provides a highly efficient gene transfer into human CB-derived hematopoietic stem cells (19). CD34+ CB cells are the youngest somatic stem cells and are expected to have no postnatal genomic aberration by irritants from the environment or UV rays. They correspond to the hematopoietic stem cells and progenitors with less epigenetic modification related to hematopoietic differentiation. These unique features of CD34+ CB cells suggest that this cell fraction might be an ideal cell source fraction for generating a gold standard iPSC. However, the risk of foreign gene integration (20, 21) needs to be overcome for future clinical applications. We successfully obtained viral/factor-free CB-iPSCs by the TS SeV vectors, and examined the advantages of using the TS SeV vector.

Results

Generation of TS SeV Vectors. The SeV RNA polymerase comprises the phosphoprotein (P) and the large protein (L), and formation of the P-L complex is required for RNA synthesis (14). Mutations in P or L have been shown to confer temperature sensitivity to the virus (22, 23). Although a conventional non-transmissible F protein-deficient (ΔF)/TS vector was demonstrated to have low cytotoxicity at temperatures above 37 °C (24), it still expressed the *GFP* gene at 39 °C, albeit at slightly lower levels (Fig. 1*B*). Thus, we generated a greater number of TS vectors using combination of known point mutations in the *P* and/or *L* genes and screened for *GFP* gene expression in infected cells

at various temperatures. The TS vectors obtained were (*i*) P2 vectors (D433A, R434A, and K437A), which contain a charge-to-alanine mutation in the L-binding domain of the P protein (22); (*ii*) TS7 vectors (Y942H, L1361C, and L1558I); (*iii*) TS13 vectors (P2 and L1558I); and (*iv*) TS15 vectors (P2, L1361C, and L1558I), as indicated in Fig. 1. In the present study, we chose to evaluate these candidate vectors with combined mutations, because a single mutation appeared to be insufficient to confer temperature sensitivity (i.e., the Y942H, L1558I, or L1361C vector). Furthermore, by using TS candidates with combined mutations, the occurrence of WT revertant, as occasionally observed in RNA viruses (14), was less likely. In contrast with the conventional SeV vector, the TS7 and TS13 vectors expressed *GFP* at 32 °C and 35 °C, and weakly at 37 °C, but not at nonpermissive temperatures of 38 °C or 39 °C. The TS15 vector exhibited greater temperature sensitivity; with this vector, *GFP* expression was barely detected at 37 °C (Fig. 1*B*). We confirmed that there was no *GFP* expression after transfection of cells with the TS7 and TS13 vectors after temperature-shift treatment to 39 °C, even when the infected cells were then cultured at 37 °C for >1 mo with several passages (Fig. 1*C*). None of the vectors was cytotoxic, and all infected cells were attached and live, with or without temperature-shift treatment. Thus, we used these TS vectors to generate human iPSCs.

Generation of Human iPSCs with TS SeV Vectors from Fibroblasts. To apply the TS vectors to generate human iPSCs, we adopted two strategies, (*i*) to replace only *c-MYC*–carrying vector and (*ii*) to replace all of the four gene-carrying SeV vector mixtures to the TS vectors. Our previous study showed that the exogenous *c-MYC* inserted between the *HN* and *L* positions in the SeV vector

(*HNL-MYC*) persisted in the infected cells longer than any other vectors carrying *OCT3/4*, *SOX2*, or *KLF4* at the top of the vectors (18+). When *c-MYC* was inserted at the 18+ position, such selective retention of the c-*MYC*–carrying vector was not observed. This was apparently due to the prolonged replication of the *HNL-MYC* vector (17). Because GFP expression with the TS vectors was relatively weak compared with that obtained using conventional vectors (Fig. 1*B*), we initially inserted *HNL-MYC* into the TS vectors so that the initial levels of expression could be restored by the polymerases supplied in trans from the other vectors (*OCT3/4*, *KLF4*, and *SOX2*). In addition, it was hoped that by using this strategy, the viral vectors might easily disappear when the remaining vector was *HNL-MYC* in the TS vector alone (Fig. 2*A*). Using these vectors at a multiplicity of infection (MOI) of 3, we obtained colonies from human fibroblast cells that were alkaline phosphatase (ALP)-positive and exhibited human embryonic stem (ES) cell-like morphology ~28 d after induction (Fig. 2*B* and Table S1). We then monitored the amount of the SeV genome present during reprogramming and cell expansion using quantitative RT-PCR (qRT-PCR). Surprisingly, replacement of the *HNL-MYC* vector into only one of the four reprogramming factor mixtures using the TS vectors resulted in a marked decrease in all viral genomes after the appearance of the iPSCs (Fig. 2*C*). As expected, expression of *c-MYC* on the TS vectors was correlated with the viral genome (Fig. S1). Then individual colonies were isolated, and the remaining SeV genome in each colony was evaluated. During cell expansion, the vectors were diluted, and most colonies were only partially positive for SeV (Fig. 2*D*, *Middle*). At passage 4, 80% of the colonies were negative for the viral genome using the TS13-
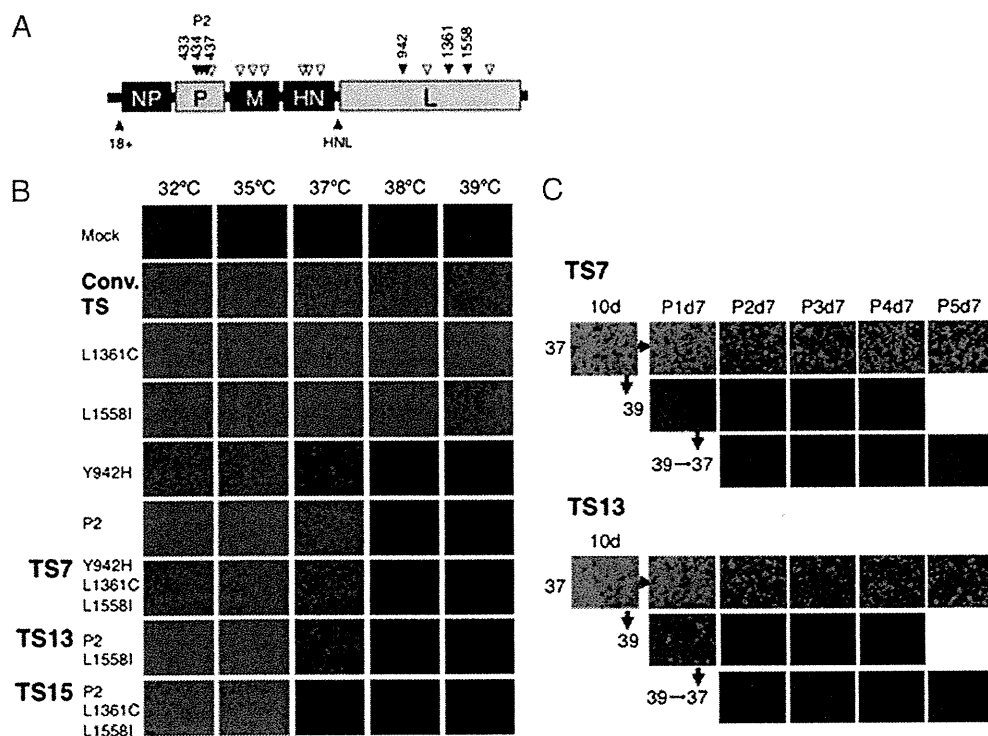
Fig. 1. Generation of TS SeV vectors and inactivation after temperature-shift treatment. (*A*) Point mutations were introduced into the polymerase-related genes *P* (P2: 433, 434, and 437) and/or *L* (942, 1361, and 1558), as indicated in the schematic structure of the ΔF/SeV vector. Open angles indicate conventional mutations in the previous TS vector; closed angles, newly introduced mutations. (*B*) Confluent LLC-MK2 cells were transduced with each SeV vector carrying *GFP* at an MOI of 5 and cultured at the indicated temperatures (32, 35, 37, 38, and 39 °C). Green fluorescence was compared at 3 d after infection. (*C*) To confirm the irreversible inactivation of gene expression by temperature-shift treatment, infected cells were cultured at 37 °C for 10 d and then split into two groups, one group cultured at 37 °C and the other cultured at 39 °C for 28 d, with cells passaged every 7 d. Similarly, cells infected with a TS vector treated at a nonpermissive temperature of 39 °C for 7 d were also cultured for a further 28 d at 37 °C, with cells passaged every 7 d, to evaluate *GFP* expression.
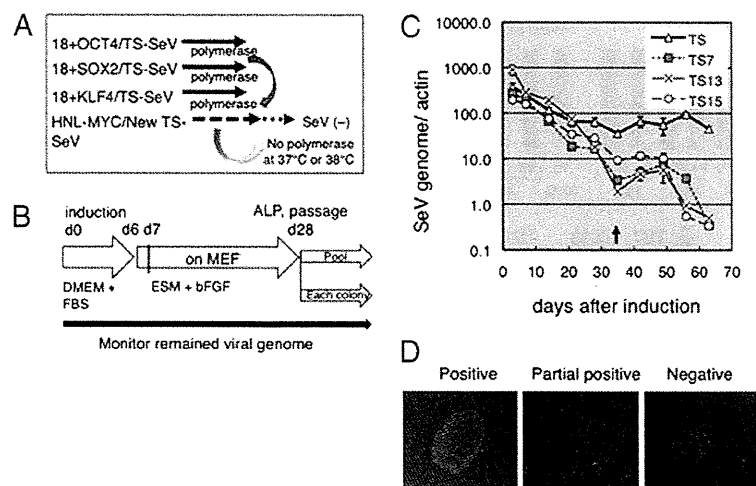
Fig. 2. (A) Strategy used to obtain vector/factor-free iPSCs with an SeV vector mixture. Human fibroblasts were infected with the SeV vector mixture containing four factors. During reprogramming, polymerases may be supplied to the TS vector (which has c-MYC at the HNL position) by OCT3/4-, SOX2-, and KLF4-carrying conventional SeV vectors. Then the SeV vector may disappear when there is TS vector alone at nonpermissive temperature. (B) Procedure for reprogramming using SeV vectors. (C) qRT-PCR of existing SeV genomes in induced cells. RNA was extracted from cells between 3 d and 2 mo after infection, and the amount of SeV genome was analyzed by qRT-PCR. iPSC colonies were passaged every 7 d after day 35 (arrow), and whole colonies on the culture dish were analyzed. (D) Typical staining of iPSC colonies with anti-SeV antibodies. (Left) At passage (P) 1, many colonies were positive for SeV. (Middle) After several passages (P4), many colonies were partially positive. (Right) Colonies were found to be negative for SeV at P10. (Scale bar: 200 μm.)

HNL-MYC and TS15-HNL-MYC vectors, and by passage 10, all colonies were negative for the vector by qRT-PCR (Fig. 3A, Left). Because the number of SeV-negative colonies was not increased using the TS7 vector at passage 10, although the partial negative colonies were increased, the iPSCs were subjected to a temperature shift to 38 °C (Fig. 3A, Right). Incubation of cells at 38 °C for 3–5 d was sufficient to obtain SeV-negative iPSCs (Figs. 3A and 4B) with no changes in the expression of human ES cell (hESC) marker genes, NANOG (Fig. 4B), or the other related marker genes. Quantitative RT-PCR analysis and Western blot analysis of these iPSCs obtained by the first strategy revealed no detectable viral genome or protein expression in the established iPSCs at the late passage numbers, with slightly detectable viral genome or protein expression in the pooled colonies at passage 8 (1/1,000–1/10,000 compared with day 3; Fig. 3 B and C and Table S3). TS15 showed higher dilution than other vectors, comparable to their temperature sensitivities. More importantly, copy numbers of OCT3/4, SOX2, KLF4, and c-MYC genes in SeV-generated iPSCs were the same as in parental cells, in contrast to retroviral-generated iPSCs, in which copy numbers were verified because of the vector integration (Fig. 3D). The condition and the efficiencies of these experiments and characteristics of obtained iPS clones are summarized in Tables S1 and S3.

Expression of Human ES Cell Markers and Epigenetics. All iPSCs examined expressed hESC markers, as determined by qRT-PCR, and were positive for stage-specific embryonic antigen (SSEA)-4, TRA-1-60, TRA-1-81, NANOG, and OCT4, as demonstrated by immunostaining (Fig. S2 A and B). Furthermore, CpG dinucleotides at the OCT3/4 promoter region in the iPSCs were demethylated (Fig. S2C). Global gene expression in the iPSCs was similar to that of hESCs (Fig. S3A). Clustering analysis revealed a high degree of similarity among the reprogrammed iPSCs obtained using the TS7, TS13, or TS15 vectors that clustered together with hESCs and was distant from that of the parental somatic cells. These iPSCs had a normal 46 XY or 46 XX karyotype, even after temperature-shift treatment, and could be maintained for more than 20 passages (Fig. S4A and Table S3). DNA fingerprinting analysis verified that these iPSCs were indeed derived from the parental fibroblast cells (Fig. S4B).

Established iPSCs Show Potentiality of Differentiation to Three Germ Layers. The ability of hESCs/iPSCs to differentiate into all cell types provides the basis for their potential in regenerative medicine. Thus, we investigated the differentiating potential of SeV-generated iPSCs by evaluating teratoma formation. In these experiments, the virus-negative iPSCs were injected s.c. or i.m. into NOD/SCID mice. Histological examination of the teratomas revealed that the tissues had originated from the three embryonic germ layers and included neural and epithelial tissues, muscle, cartilage, bone, gut-like structures, and various glandular structures (Fig. S3B). We further tested the pluripotency of SeV-generated iPSCs in vitro. Like hESCs, these iPSCs formed embryoid bodies in suspension culture (Fig. S4C). For mesoderm-derived differentiation, the embryoid bodies were grown in adherent culture with 0.1 mM ascorbic acid and 20% FBS to enhance cardiomyocyte differentiation (25), whereas an established protocol for hESCs involving activin A treatment (26) was used for the induction of definitive endoderm cells. As a result, SeV-generated iPSCs differentiated into beating cardiomyocytes and endoderm-derived pancreatic cells that stained positive for pancreatic and duodenal homeobox 1 (PDX1; Fig. S4C). Coculture of these iPSCs with PA6 feeder cells resulted in the generation of dopaminergic neurons (ectoderm derivatives) that were positive for βIII tubulin and tyrosine hydroxylase (27) (Fig. S4C). These data indicate that the SeV-generated iPSCs are pluripotent, like hESCs, and respond to different differentiation stimuli. Based on these results, we conclude that the viral/factor-free iPSCs generated using TS SeV vectors meet the criteria of hESCs and could serve as a clinically important source of stem cells without the danger of integration of any foreign genes.

Generation of Human iPSCs from CB Cells. In the second strategy, we obtained viral-free iPSCs from human fibroblasts using TS13 or TS7 vector mixtures consisting of four reprogramming factors (i.e., 4F/TS13 and 4F/TS7, respectively) at a higher MOI of 30 at 37 °C, with (TS7) or without (TS13) temperature-shift treatment (Fig. 4A and B and Table S1). In this case, we used a higher MOI because we could not obtain iPSCs at a lower MOI, likely due to the weak expression of TS vectors at 37 °C, lacking any supplemental polymerases from mixed conventional vectors. However,
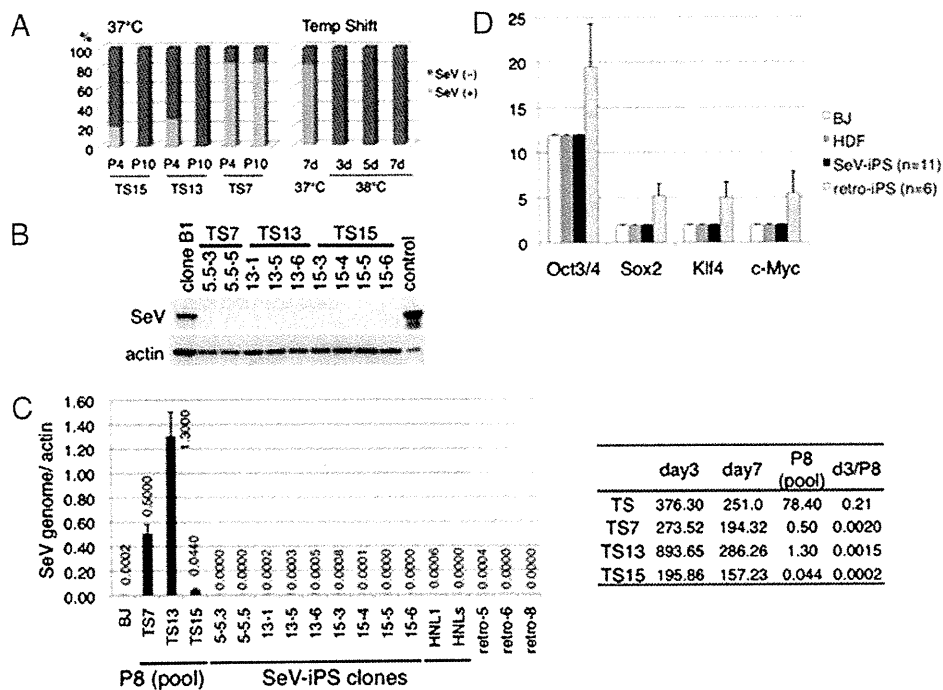
Fig. 3. (A) Ratio of SeV-positive colonies. P, passage number. (Left) Randomly chosen colonies were expanded independently, and the existence of SeV vectors was evaluated by qRT-PCR at P4 and P10. The number of positive and negative colonies was counted and is expressed for each as a ratio of all colonies chosen (n = 12 per each TS vector). (Right) Temperature shift to a nonpermissive temperature of 38 °C effectively removed SeV vectors from the iPSC colonies generated using TS7 vectors. The culture dishes at P4 were split and transferred to culture at 37 or 38 °C for the number of days indicated. The ratio was calculated as left panel. (B) SeV proteins were not detected in iPSC colonies by Western blot analysis with anti-SeV antibodies. Clone B1, positive control for iPSCs in which the SeV persisted (17); control, LLC-MK2 cells transfected with plasmids encoding SeV vectors. 5.5-3 and 5.5-5 were generated with MYC/TS7; 13-1, 13-5, and 13-6 were generated with MYC/TS13; and 15-3, 15-4, 15-5, and 15-6 were generated with MYC/TS15. (C) qRT-PCR of viral genome in SeV-generated iPSCs (viral genome/actin). BJ, parental fibroblasts; day 3 and day 7, BJ cells infected with SeV vectors after 3 and 7 d; HNL1 and HNLs, iPSCs established using conventional SeV (17). P8, pooled colonies at passage 8. Values <0.001 were backgrounds under the calculation curve as detected in parental cells. (D) Copy numbers of OCT3/4, SOX2, KLF4, and c-MYC in parental cells [BJ and human dermal fibroblast (HDF) cells] and iPSCs generated by SeV (SeV-iPS; n = 11) or retrovirus (retro-iPS; n = 6), as determined by qRT-PCR of genomic DNA. The passage numbers of tested clones are listed in Table S3.

an MOI of only 2 was sufficient to generate iPSCs from the CB cells described below, possibly because of the highly efficient gene transfer into human CB stem cells (19). We infected freshly isolated mononuclear cells with the GFP construct at an MOI of 2 and found that GFP expression was limited to the CD34$^+$ fraction (43% of the CD34$^+$ cells were GFP$^+$ cells), whereas no GFP$^+$ cells were found in the CD34$^-$ fraction at 2 d after SeV infection (19). The rate of SeV infection determined by GFP expression in CD34$^+$ cells was increased up to 100% if we used SeV vectors at an MOI of 20. This fraction corresponds to hematopoietic stem cells or progenitors, as reported elsewhere (28). Then freshly isolated purified CD34$^+$ CB cells (purity of CD34$^+$, 96–99%) or the frozen CD34$^+$ CB cells (RIKEN BioResource Center; purity of CD34$^+$, 97–99%), thawed 1 d before infection, were used for SeV infection. These cells were treated with a SeV vector mixture consisting of SeV TS7-OCT3/4, -SOX2, -KLF4, and -c-MYC. Infected cells were incubated under hematopoietic cell culture conditions, followed by cocultivation on mitomycin C (MMC)-treated SNL cells on day 4 or day 10 (Fig. 4C). hESC-like colonies expressing SSEA-4 appeared after 14 d of cocultivation with SNL (18 d after SeV infection), whereas no colonies were obtained after transfer onto SNL on day 10 (Table S2). The efficiency with which iPSC colonies emerged on SNL feeder cells using SeV TS7 vectors is also shown in Table S2. To eliminate remaining SeV virus constructs, ESC-like colonies were subjected to heat treatment at 38 °C for 3 d and recloned. SeV-positive cells constituted 60–80% of total cells within hESC-like colonies before heat treatment (clones SeV iPSC 4, 15, and 17; passage 2).

This was reduced to 0% after recloning (clones SeV iPSC 4A, 15A, and 17A; passage 4), followed by the heat treatment. The percentages of SeV-positive cells were determined by the proportion of sum of the area positively detected with anti-SeV HN (envelope) antibody against total colony area. In the agreement with this staining result, SeV constructs were not detected by qRT-PCR at passage 4 after heat treatment (Fig. 4E). The virus-negative ESC-like clones showed the expression of hESC markers (Fig. S5 A and B), global gene expression profile similar to that of hESCs (Fig. S5 C and E), and normal karyotype (Fig. S5D). Seven established cell clones were tested for embryoid body–mediated in vitro differentiation potential, and three out of the seven clones were found to have in vivo differentiation potential in a teratoma formation assay with SCID mice. All three of these clones were able to give rise to cells of all three germ layers as detected by immunocytochemistry and cell morphology studies (Fig. S5F). These three lines formed the teratomas with a cystic mass containing differentiated tissues morphologically corresponding to all three germ layers (Fig. S5F). The characterization of established clones from fibroblasts and CB cells is summarized in Table S3.

Discussion

The present study has demonstrated that the established TS SeV vectors TS15, TS13, and TS7 are highly effective tools with which we were able to obtain transgene-free human iPSCs. These iPSCs were generated efficiently by robust gene replication, with a subsequent rapid decrease in the level of factor-carrying SeV vectors
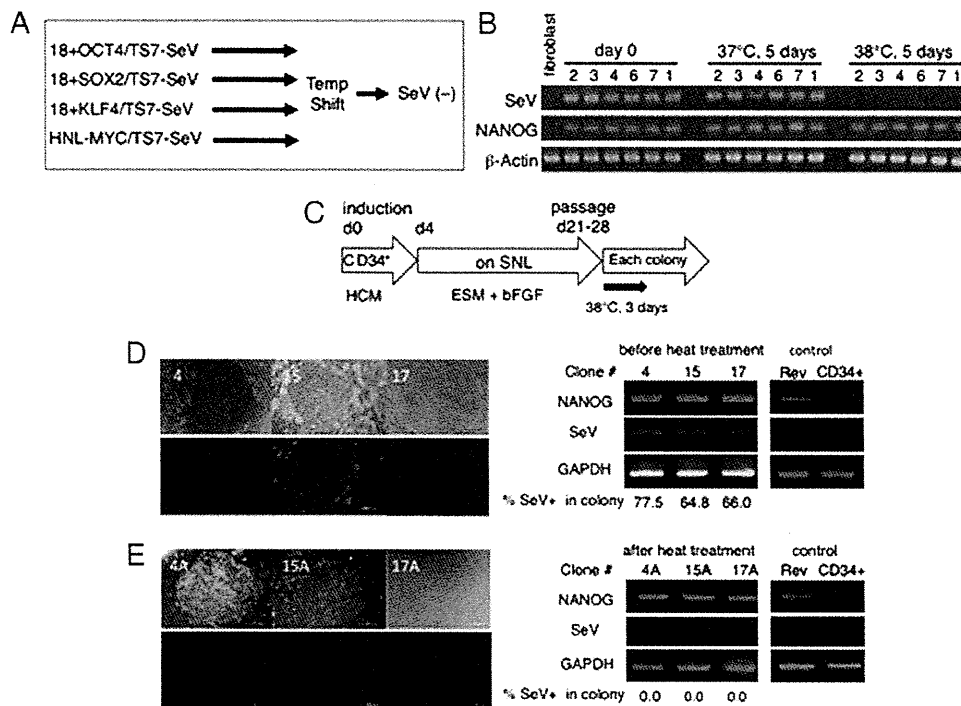
Fig. 4. Our second strategy with temperature-shift treatment. (A) Schemes to remove viral genome. (B) qRT-PCR of the SeV genome and hESC markers before and after temperature-shift treatment. iPSCs generated from HDF cells using TS7 vectors were treated with a temperature shift to 38 °C for 5 d. The SeV genome was not detected after this temperature-shift treatment, whereas expression of *NANOG* was not affected. (C) Schemes for generation of virus vector-free iPSCs from CD34⁺ CB cells with SeV vectors. The ESC-like colonies 4, 15, and 17 that emerged were subcloned after heat treatment for 3 d at 38 °C. (D and E) The remaining SeV construct in SeV iPSC 4, SeV iPSC 15, and SeV iPSC 17 (D; passage 2, before heat treatment) and heat-treated subclone SeV iPSC 4A (from 4), SeV iPSC 15A (from 15), and SeV iPSC 17A (from 17) (E; passage 4) were determined by immunostaining with anti-HN antibody (*Left*) and by qRT-PCR against endogenous *NANOG* transcript and SeV RNA construct (*Right*). Retrovirally generated iPSCs from CB cells (Rev) and CD34⁺ CB cells (CD34) were used as controls. The percentage of SeV-positive cells in the respective colony was determined using a two-value recognition function and is given below the qRT-PCR image.

during cell expansion (Fig. 2C). Almost all of the colonies picked up were virus-negative at late passages, and even if vectors were present, they could be easily removed using the temperature-shift protocol (Figs. 3A and 4). Indeed, the iPSCs generated using TS SeV vectors were free of any integrated viral factors, in contrast to retroviral-generated iPSCs, which express variable copy numbers of *OCT3/4*, *SOX2*, *KLF4*, and *c-MYC* (Fig. 3D). We also demonstrated that using TS SeV vectors, virus-negative iPSCs were efficiently generated from CD34⁺ human CB cells (Fig. 4).

Although the use of synthetic modified mRNA to generate iPSCs has been reported, this is highly dependent on the gene delivery system, because it requires repetitive transfection for 16 d (13). Therefore, it might not be applicable to difficult-to-transfect cells, such as primary peripheral blood cells. The addition of decoy receptor to prevent IFN production by host cells is also needed. In contrast, SeV vectors require no transfection reagents or decoy receptors. We suggest that this is a considerable advantage to using nonintegrating SeV; the iPSCs thus generated have a homogeneous genetic background. Several studies on the generation of iPSCs from blood cells and CB cells with integration-free episomal vectors have been published recently (29–31). The efficiency of generating iPSCs is lower with episomal vectors than with SeV (>0.1% at an MOI of 2) and varies depending on the construction of the vectors and the nature of the transfection medium used. The major advantage of using nonintegrated SeV vectors is a potent and robust protein-expressing property that does not require optimization of the transfection medium. The volume of collected CB is 80–120 mL and may contain 2–4 × 10⁵ CD34⁺ cells on average. Our results show that only 1 × 10⁴ CD34⁺ cells, corresponding to ~5 mL of

CB, are needed to obtain 10 independent iPSC clones with SeV. The rest of the CB can be sorted and used for the regular bone marrow transplantation therapy. In addition, there have been no reports of pathogenicity associated with SeV in primates, and the safety of the SeV vector is further enhanced by the F-deficiency that makes the vector nontransmissible (16).

In the present study, we have confirmed that the SeV vectors were not reactivated or detected in iPSCs at late passages or after temperature-shift treatment (Figs. 1C and 3). It has been suggested that TS mutations in P and L affect polymerase activity and promote degradation of the virus vector after treatment at nonpermissive temperatures (23). Based on our findings, we believe the TS SeV vector system that allows the elimination of remaining SeV construct from reprogrammed cells by temperature-shift treatment could accelerate future clinical application of iPSCs generated from cells obtained by less invasive or even noninvasive methods.

Materials and Methods

The induction of human iPSCs was done as reported previously (1, 17). Unless indicated otherwise, SeV vectors (*OCT3/4*, *SOX2*, *KLF4*, and *c-MYC*) were used at an MOI of 3 or 30 for 1 × 10⁶ fibroblasts. For retroviral induction, fibroblasts were infected with mCAT containing simian immunodeficiency virus (SIV) vector at an MOI of 50, and then expanded by induction with retrovirus vectors containing reprogramming factors. Infected cells were transferred onto MMC-treated mouse embryonic fibroblast (MEF) feeder cells on day 6 after induction. Details of the experimental procedures are provided in *SI Materials and Methods*.

1. Takahashi K, et al. (2007) Induction of pluripotent stem cells from adult human fibroblasts by defined factors. *Cell* 131:861–872.
2. Yu J, et al. (2007) Induced pluripotent stem cell lines derived from human somatic cells. *Science* 318:1917–1920.
3. Okita K, Nakagawa M, Hyenjong H, Ichisaka T, Yamanaka S (2008) Generation of mouse-induced pluripotent stem cells without viral vectors. *Science* 322:949–953.
4. Yu J, et al. (2009) Human induced pluripotent stem cells free of vector and transgene sequences. *Science* 324:797–801.
5. Soldner F, et al. (2009) Parkinson's disease patient–derived induced pluripotent stem cells free of viral reprogramming factors. *Cell* 136:964–977.
6. Sommer CA, et al. (2009) Induced pluripotent stem cell generation using a single lentiviral stem cell cassette. *Stem Cells* 27:543–549.
7. Stadtfeld M, Nagaya M, Utikal J, Weir G, Hochedlinger K (2008) Induced pluripotent stem cells generated without viral integration. *Science* 322:945–949.
8. Woltjen K, et al. (2009) piggyBac transposition reprograms fibroblasts to induced pluripotent stem cells. *Nature* 458:766–770.
9. Kaji K, et al. (2009) Virus-free induction of pluripotency and subsequent excision of reprogramming factors. *Nature* 458:771–775.
10. Jia F, et al. (2010) A nonviral minicircle vector for deriving human iPS cells. *Nat Methods* 7:197–199.
11. Zhou H, et al. (2009) Generation of induced pluripotent stem cells using recombinant proteins. *Cell Stem Cell* 4:381–384.
12. Kim D, et al. (2009) Generation of human induced pluripotent stem cells by direct delivery of reprogramming proteins. *Cell Stem Cell* 4:472–476.
13. Warren L, et al. (2010) Highly efficient reprogramming to pluripotency and directed differentiation of human cells with synthetic modified mRNA. *Cell Stem Cell* 7:618–630.
14. Lamb RA, Kolakofsky D (1996) Paramyxoviridae: The viruses and their replication. Fields Virology, eds Fields BN, Knipe DM, Howley PM (Lippincott-Raven, Philadelphia), 3rd Ed, pp 1177–1204.
15. Li HO, et al. (2000) A cytoplasmic RNA vector derived from nontransmissible Sendai virus with efficient gene transfer and expression. *J Virol* 74:6564–6569.
16. Nagai Y, Takakura A, Irie T, Yonemitsu M, Gotoh B (2011) Evolution of Sendai virus: The journey from mouse pathogen to a state-of-the-art tool in virus research and biotechnology. The Paramyxoviruses, ed Samal SK (Horizon Scientific Press, Norwich, UK).

17. Fusaki N, Ban H, Nishiyama A, Saeki K, Hasegawa M (2009) Efficient induction of transgene-free human pluripotent stem cells using a vector based on Sendai virus, an RNA virus that does not integrate into the host genome. *Proc Jpn Acad, Ser B, Phys Biol Sci* 85:348–362.
18. Seki T, et al. (2010) Generation of induced pluripotent stem cells from human terminally differentiated circulating T cells. *Cell Stem Cell* 7:11–14.
19. Jin CH, et al. (2003) Recombinant Sendai virus provides a highly efficient gene transfer into human cord blood–derived hematopoietic stem cells. *Gene Ther* 10:272–277.
20. Giorgetti A, et al. (2009) Generation of induced pluripotent stem cells from human cord blood using OCT4 and SOX2. *Cell Stem Cell* 5:353–357.
21. Takenaka C, Nishishita N, Takada N, Jakt LM, Kawamata S (2010) Effective generation of iPS cells from CD34⁺ cord blood cells by inhibition of p53. *Exp Hematol* 38:154–162.
22. Bowman MC, Smallwood S, Moyer SA (1999) Dissection of individual functions of the Sendai virus phosphoprotein in transcription. *J Virol* 73:6474–6483.
23. Feller JA, Smallwood S, Skiadopoulos MH, Murphy BR, Moyer SA (2000) Comparison of identical temperature-sensitive mutations in the L polymerase proteins of Sendai and parainfluenza3 viruses. *Virology* 276:190–201.
24. Inoue M, et al. (2003) Nontransmissible virus-like particle formation by F-deficient Sendai virus is temperature-sensitive and reduced by mutations in M and HN proteins. *J Virol* 77:3238–3246.
25. Guo XM, et al. (2006) Creation of engineered cardiac tissue in vitro from mouse embryonic stem cells. *Circulation* 113:2229–2237.
26. D'Amour KA, et al. (2005) Efficient differentiation of human embryonic stem cells to definitive endoderm. *Nat Biotechnol* 23:1534–1541.
27. Kawasaki H, et al. (2000) Induction of midbrain dopaminergic neurons from ES cells by stromal cell–derived inducing activity. *Neuron* 28:31–40.
28. Majeti R, Park CY, Weissman IL (2007) Identification of a hierarchy of multipotent hematopoietic progenitors in human cord blood. *Cell Stem Cell* 1:635–645.
29. Chou BK, et al. (2011) Efficient human iPS cell derivation by a non-integrating plasmid from blood cells with unique epigenetic and gene expression signatures. *Cell Res* 21:518–529.
30. Hu K, et al. (2011) Efficient generation of transgene-free induced pluripotent stem cells from normal and neoplastic bone marrow and cord blood mononuclear cells. *Blood* 117:e109–e119.
31. Yu J, Chau KF, Vodyanik MA, Jiang J, Jiang Y (2011) Efficient feeder-free episomal reprogramming with small molecules. *PLoS ONE* 6:e17557.
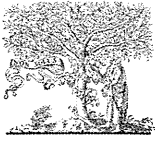
MEDICAL SCIENCES
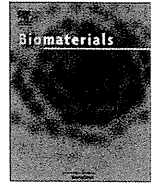
The use of leukemia inhibitory factor immobilized on virus-derived polyhedra to support the proliferation of mouse embryonic and induced pluripotent stem cells

Naoki Nishishita [a,b,1], Hiroshi Ijiri [c,1], Chiemi Takenaka [a,b], Kenichiro Kobayashi [b], Kohei Goto [c], Eiji Kotani [c], Tohru Itoh [d], Hajime Mori [c,e,**], Shin Kawamata [a,b,*]

[a] Foundation for Biomedical Research and Innovation TRI308, 1-5-4 Minatojima-Minamimachi, Chuo-ku, Kobe 650-0043, Japan
[b] Riken Center for Developmental Biology, 2-2-3 Minatojima-Minamimachi, Chuo-ku, Kobe 650-0047, Japan
[c] Insect Biomedical Research Center, Kyoto Institute of Technology, Matsugasaki, Sakyo-ku, Kyoto 606-8585, Japan
[d] TC Reagent Group, Consumer Products Division, Production General Division, AGC Techno Glass Co., Ltd., 1-50-1 Gyoda, Funabashi 273-0044, Japan
[e] Protein Crystal Corporation, 1-12-8 Senba Higashi, Minoh 541-0053, Japan

ARTICLE INFO

ABSTRACT

Human leukemia inhibitory factor (LIF) was immobilized into insect virus-derived microcrystals (polyhedra) to generate LIF polyhedra (LIF-PH) that can slowly release LIF into embryonic stem (ES) cell culture media and thus maintain ES cells in an undifferentiated state. Assays of the biological activities of LIF-PH indicated that a single addition of LIF-PH to the ES cell culture medium can support the proliferation of mouse ES and induced pluripotent stem (iPS) cells continuously for 14 days, and suggest that LIF-PH can be successfully used in the place of a periodic addition of recombinant LIF to the media every 2–3 days. The release of LIF protein from LIF-PH was determined by enzyme-linked immunosorbent assay (ELISA). Maintenance of undifferentiated state of mouse ES and iPS cells cultured with LIF-PH was determined by the detection of pluripotency-related biomarkers Oct3/4 and stage-specific embryonic antigen-1 (SSEA-1) through immunostaining and measurement of alkaline phosphatase activity. In this paper, we propose a closed culture system for mass production of ES and iPS cells that utilize a slow-releasing agent of LIF.

1. Introduction

Leukemia inhibitory factor (LIF) initially was identified as a cytokine capable of inducing the differentiation of M1 myeloid leukemia cells, and later was shown to have a strong differentiation-inhibiting activity on embryonic stem (ES) cells [1,2]. At present, mouse ES cells are cultured in an undifferentiated state on gelatin-coated polystyrene plates in the presence of LIF [3,4]. LIF belongs to the family of interleukin-6 (IL-6)-type cytokines. This family of cytokines stimulates target cells through the gp130 receptor, which is expressed in all cells of the body, while the specific cytokine receptor subunits are expressed in a cell-specific manner and induce a specific cellular response when triggered by a particular member of the cytokine family. LIF induces heterodimerization of the gp130 and LIF receptor (LIFR) upon binding to receptor subunits, and this dimerization results in the activation of associated Jak tyrosine kinases and initiation of intracellular signaling cascades [5]. Jak-mediated phosphorylation of specific tyrosine residues in the gp130 cytoplasmic domain creates docking sites for Src homology 2-containing signal transducer and activator of transcription (STAT) proteins, which are then phosphorylated and translocate to the nucleus as dimers to induce expression of specific sets of genes [6,7]. The STAT protein family has seven members, of which STAT3 is the major mediator of gp130 signals [8]. STAT3 is thought to be involved in the induction of a set of genes related to maintenance of pluripotency and self-renewal in ES cells [9,10]. Previous reports indicate that mouse LIF binding activity is specific to mouse LIFR, while human LIF can bind LIFR from either human or mouse. In addition, the binding activity of human LIF to mouse LIFR is higher than that of mouse LIF [11,12].

The disruption or removal of LIF signaling (e.g. by cytokine starvation) will trigger a signal within stem cells to differentiate [13]. Presumably, continuous activation of LIF-mediated signaling by a slow, steady release of LIF in cell culture, rather than spikes in activation and rapid withdrawal of LIF-mediated signaling observed

during periodic addition of recombinant LIF would be beneficial for maintaining stem cell pluripotency during self-renewal. For this purpose, we have developed a new slow-releasing agent comprised of a viral protein crystalline matrix containing immobilized human LIF molecules.

Cypovirus (CPV) infections of insect larvae are characterized by the production of massive amounts of a major virus-encoded protein (polyhedrin). The polyhedrin protein molecules crystallize in the cell cytoplasm to form cubic inclusion bodies (polyhedra) that incorporate numerous virus particles. CPVs belong to a genus within the *Reoviridae* family [14]. Polyhedra function to facilitate the survival of the incorporated virus in hostile environments, stabilizing the virions and allowing long-term viability. These polyhedra are also highly resistant to both nonionic and ionic detergents and are soluble at neutral pH [15]. Previously, we have produced recombinant polyhedra derived from *Bombyx mori* cypovirus (BmCPV) without incorporation of virus particles. We developed two targeting strategies for the incorporation of foreign proteins into polyhedra. Diverse foreign proteins can be immobilized into polyhedra by fusing a polyhedron-targeting tag sequence at the C- or N-terminus of the foreign protein [16].

As described in this report, we have generated two types of polyhedra by immobilizing human LIF fused with a polyhedron-targeting tag sequence at either the C- or N-terminus. The biological effects of these polyhedra on cultured stem cells were determined and compared to those effects seen when using recombinant human LIF (rhLIF) in analogous experiments.

2. Materials and methods

2.1. Generation of LIF polyhedra

Recombinant LIF baculovirus transfer vectors were generated using GATEWAY® cloning technology (Invitrogen). The LIF gene fused to DNA encoding either the VP3 or the H1 immobilization signal was amplified by polymerase chain reaction (PCR) using primer sets containing *att*B1 and *att*B2 sequences. The forward primer 5′-GGGGACAAGTTTGTACAAAAAAGCAGGCTTAATGAAGGTCTTGGCGGCAGGAG-3′ and reverse primer 5′-GGGGACCACTTTGTACAAGAAAGCTGGGTAGAAGGCCTGGGCCAA-CACGGCG-3′ were used to amplify the LIF gene coupled to DNA encoding the VP3 immobilization signal, and the forward primer 5′-GGGGACAAGTTTGTACAAAAAA-GCAGGCTTAAAGGTCTTGGCGGCAGGAGTTG-3′ and reverse primer 5′-GGGGAC-CACTTTGTACAAGAAAGCTGGGTGCTAGAAGGCCTGGGCCAACACGGCG-3′ were used to amplify the LIF gene fused to DNA encoding the H1 immobilization signal. The resulting *att*B-flanked PCR products were cloned into a donor vector (pDONR221) by BP reactions of GATEWAY® system. To produce transfer vectors encoding H1 or VP3 immobilization signals, the open reading frame cloned between the *att*L1 and *att*L2 sites in the entry vectors was transferred to destination vectors (pDEST-C-VP3 or pDEST-N-H1) via LR Clonase™ reactions. The resulting transfer vectors were co-transfected into *Spodoptera frugiperda* IPLB-Sf21-AE (Sf21) cells with linearized Baculogold Baculovirus DNA (BD Pharmingen), and replication-competent baculovirus was rescued by recombination between transfer vector and the linearized viral DNA and ultimately harvested from the supernatant. Immobilization of LIF using VP3 or H1 signals was accomplished by dual infection of the recombinant baculoviruses that express the LIF fusion proteins and a recombinant baculovirus AcCP-H expressing BmCPV polyhedrin. The resulting polyhedra were recovered and purified from Sf21 cells, and detected by western blotting as previous reported in Reference [16]. Polyhedra were stored in distilled water containing penicillin (100 U/mL) and streptomycin (100 µg/mL).

2.2. Cell culture

The mouse ES cell line, EB5, was derived from *E14tg2a* (ATCC) by inserting the *Aspergillus terreus* blasticidin S deaminase gene and was provided by Dr. Niwa (Riken CDB, Kobe), and maintained as previously described in References [3,4]. In brief, EB5 cells were maintained on 6-well plates (Asahi Glass) coated with 0.1% type A gelatin (Sigma–Aldrich) in undifferentiation medium ["glow minimum essential medium" (GMEM; Invitrogen) supplemented with 1% fetal bovine serum (FBS; CELLect, MP Bioscience), 10% KnockOut Serum Replacement (KSR; Invitrogen), 0.1 mM nonessential amino acids (NEAA; Invitrogen), 1 mM sodium pyruvate (Invitrogen), 0.1 mM 2-mercaptoethanol, blasticidin (500 ng/mL; Invitrogen), and 2000 U/mL (10 ng/mL) rhLIF (Chemicon International LIF1005)]. Cultivation of undifferentiated EB5 cells harboring a blasticidin resistant gene that is fused to the *Oct-4* promoter region was achieved through blasticidin selection. EB5 passaging was accomplished by washing

cells once with phosphate-buffered saline (PBS) and then incubating with 0.05% trypsin-ethylenediaminetetraacetic acid (EDTA) at 37 °C for 5 min. Cell clumps were dissociated completely by pipetting in undifferentiation medium. Ten thousand cells were seeded in a 6-well plate and cultured in 2 mL of undifferentiation medium for 3 days before the next passage.

To generate mouse iPS cells, neural stem cells (NSCs) isolated from Oct-4/green fluorescent protein (GFP) transgenic mice [17] were used as cell source for reprogramming. One hundred thousand NSCs were transduced with retroviruses bearing c-*Myc*, *Klf4*, *Oct3/4* and *Sox2* genes as described in Reference [18]. Twenty-four hours post-transduction, cells were transferred to ES medium and maintained in feeder-free gelatin-coated plates. Oct-4-GFP positive cells emerged within 1 week and iPS cells (IWF-1; named after iPSc Without Feeder cell) were established in 3 weeks. Silencing of the exogenous factor and reactivation of the series of endogenous pluripotency markers were confirmed by reverse transcription (RT)-PCR. Generation of chimeric mice was confirmed following blastocyst injection.

2.3. Cell proliferation assay

For both short-term (7 days) and for long-term culture (14 days) culture, 2×10^5 cubes or 5×10^5 cubes of polyhedra containing either H1-tagged LIF (H1/LIF polyhedra) or VP3-tagged LIF (LIF/VP3 polyhedra) were mixed in 0.1% gelatin solution, coated on a polystyrene plate, and air-dried at room temperature. Cells were harvested and counted at indicated days.

2.4. Immunostaining of ES cell undifferentiation markers

Mouse ES or iPS cells were cultured with either 2×10^5 cubes of H1/LIF polyhedra, LIF/VP3 polyhedra, empty polyhedra (CP-H polyhedra), 10 ng/mL of rhLIF, or without rhLIF in the absence of blasticidin for 3 days. Cells were then fixed in 4% paraformaldehyde in permeabilization solution (0.2% Triton X-100 in PBS) for 20 min at 4 °C, rinsed with PBS, and then blocked in a blocking buffer (PBS containing 0.1% bovine serum albumin (BSA)) for 15 min at room temperature. The ES cells were incubated with a 1:100 dilution of primary antibody against Oct-4 (Santa Cruz Biotechnology, catalog #SC-5279) or against stage-specific embryonic antigen-1 (SSEA-1; Santa Cruz Biotechnology, catalog #SC-21702), and mouse iPS cells were incubated with primary antibody against SSEA-1 at 4 °C overnight followed by incubation with Alexa fluorophores (Invitrogen) for 1 h at 37 °C. Alkaline phosphatase (ALP) activity of cultured cells was detected with a Vector Blue® Alkaline Phosphatase Subtraction Kit (Vector Laboratories) according to the manufacturer's instructions. Cells were observed by either fluorescence microscopy or by phase-contrast microscopy using an Olympus CKX-31 inverted microscope.

2.5. Enzyme-linked immunosorbent assay (ELISA)

Concentration of LIF in culture media was determined by ELISA. Two hundred thousand cubes of CP-H polyhedra or either LIF/VP3 or H1/LIF polyhedra were added in undifferentiation medium to 1×10^5 EB5 cells. The release of LIF from polyhedra in fresh undifferentiation medium was measured at days 0 (1 h after adding polyhedra to the cell culture), 1, 2, 3, 4 or 5, and was determined using a Human LIF Quantikine ELISA kit (R&D Systems) in accordance with the manufacturer's protocol. The release of LIF from polyhedra in a conditioned medium harvested from culture medium used to keep EB5 in confluence for 24 h was also determined with this kit. The amount of soluble LIF was measured by absorbance at 450 nm with a microplate reader (Model 680, Bio-Rad).

Activation of STAT3 was also determined by ELISA. Ten thousand EB5 cells were cultured without rhLIF in the presence of blasticidin for 3 days to generate a LIF starvation culture, and then either 2×10^6 cubes of H1/LIF polyhedra or 10 ng/mL rhLIF was added to the cell culture. The cells were harvested at designated time points, mixed with ice-cold cell lysis buffer (Cell Lysis Buffer (10×); Cell Signaling) with 1 mM phenylmethylsulfonyl fluoride (PMSF; Sigma) and incubated at 4 °C for 5 min after assessing the cell number. The cell lysate was centrifuged at 14000×g for 10 min at 4 °C, and the supernatant was then collected. Soluble phospho-STAT3 (Y705) levels in the supernatant were measured by ELISA using a PathScan® plate in accordance with the manufacturer's protocol. Horse radish peroxidase (HRP)-conjugated antibody was used for the detection of phospho-STAT3, and absorbance at 450 nm was measured with a microplate reader (Model 680, Bio-Rad).

2.6. Western blotting

Analysis by sodium dodecyl sulfate-polyacrylamide gel electrophoresis (SDS-PAGE) and western blot detection was performed by suspending 4×10^5 cubes of each type of polyhedra in 30 µL of SDS-PAGE sample buffer (50 mM Tris–HCl (pH 6.8), 100 mM dithiothreitol, 2% SDS, 0.1% bromophenol blue, and 10% glycerol), followed by boiling for 5 min, cooling on ice, and separating the polyhedra lysates by SDS-PAGE at 25 mA. Duplicate lanes for each polyhedra sample were prepared, and following electrophoresis one-half of the gel was transferred onto a nitrocellulose membrane at 54 mA for 90 min for western blotting while the other half was stained with coomassie blue. The blotted membrane was incubated with an anti-human LIF monoclonal primary antibody (R&D systems) diluted 1:250 in 3% skim milk/Tris-buffered

saline with Tween-20 (TBS-T) for 2 h at 25 °C, followed by a second incubation at 25 °C for 2 h with an HRP-conjugated anti-mouse secondary antibody (Bio-Rad) diluted 1:3000 in 3% skim milk/TBS-T. After several washes, the membrane was developed with an immunostaining kit (HRP-1000; Konica) according to the manufacturer's instructions.

3. Results

3.1. Immobilization of human LIF into BmCPV polyhedra

The viral protein VP3 mediates incorporation of BmCPV into polyhedra, and a stretch of 52 amino acids within this protein is sufficient to direct immobilization of foreign proteins into polyhedra. This 52-aa sequence was fused to the C-terminus of LIF to direct LIF uptake into polyhedra, and is termed VP3-tag. Similarly, a stretch of 30 amino acids from the N-terminal alpha helix of the BmCPV polyhedrin protein can be used to direct immobilization of foreign proteins into the cubic polyhedra structure [15,16,19], and this 30-aa sequence (termed H1-tag) was fused to the N-terminus of LIF to direct LIF immobilization into polyhedra. Human LIF protein bearing either a VP3-tag or a H1-tag was immobilized into polyhedra to generate two types of LIF polyhedra that can slowly release LIF into the culture medium, namely H1/LIF polyhedra and LIF/VP3 polyhedra. The amount of immobilized LIF, the LIF release rate from polyhedra, and the biological activities of the released protein were examined in biological assays, with the two tagging methods yielding differing outcomes.

The schema for generation of the two types of LIF polyhedra and photos of LIF polyhedra are shown in Fig. 1A. Immobilization of LIF protein into polyhedra was confirmed by the detection of LIF protein by western blotting (Fig. 1B). LIF protein can be immobilized into polyhedra by either the H1-tag or the VP3-tag. However, the intensity of LIF bands in the western blot indicates that LIF protein was more efficiently immobilized into polyhedra when the H1-tag was used.

3.2. Release of LIF in cell culture media

Release of LIF from H1/LIF and LIF/VP3 polyhedra in culture medium was determined by ELISA. Ten thousand EB5 cells were cultured with 2×10^5 cubes of H1/LIF polyhedra, and release of LIF was observed 1 h after the culture was initiated (day 0). However, the same dose of LIF/VP3 polyhedra did not release detectable levels of LIF, with measurements showing only background-level signals, as low as empty polyhedra (CP-H polyhedra) derived from an infection of Sf21 cells with AcCP-H alone (Fig. 2). The release of LIF from H1/LIF polyhedra peaked 2 days after the culture was initiated, and lasted as long as 5 days so far measured. On the other hand, rhLIF levels begin to diminish at day 3 and are drastically reduced at day 4 days, with levels almost 1/10 of the initial dose. The rhLIF levels were barely detectable at day 6. Interestingly, the amount of rhLIF added to the cell culture is drastically reduced within 1 h. A likely explanation for this drop is that some portion of rhLIF binds to LIF receptor, while the majority of rhLIF molecules stick to the wall of culture dishes or are degraded soon after addition to the cell culture media. The release of LIF was observed within 1 h when H1/LIF polyhedra were soaked in fresh cell culture media (without cells), but not in PBS (Fig. 2). Also interestingly, the amount of LIF released was suppressed when H1/LIF polyhedra were incubated with conditioned media alone (without cells) or added to overgrown EB5 cell culture that had been cultured with mouse recombinant LIF. The ELISA kit used in these studies detects rhLIF but not mouse recombinant LIF (data not shown). These data suggest that the culture media may contain substance(s) that promotes the degradation of polyhedra, while the conditioned media may have factor(s) that antagonize or neutralize such putative digestive activities of substance(s) found in fresh culture media.

3.3. Maintenance of pluripotent stem cells with H1/LIF polyhedra

Colonies of pluripotent mouse ES or iPS cells having a dome-like morphology require a continuous supply of LIF to proliferate in the undifferentiated state, while the colonies start to differentiate and become flat or take on an epithelium-like appearance in the absence of LIF. EB5 cells cultured with rhLIF or on H1/LIF or LIF/VP3 polyhedra-coated 6-well plates are shown in Fig. 3. Notably, the cell culture with 2×10^5 cubes of H1/LIF polyhedra, as well as that with 10 ng/mL rhLIF, maintained dome-shape colonies that were positively-stained with ALP, but such findings from the culture with the same dose of LIF/VP3 polyhedra were not observed (Fig. 3). In accord with the LIF release data shown in Fig. 2, these results suggest that the level of LIF release from LIF/VP3 polyhedra was not sufficient to maintain the undifferentiated state of mouse ES or iPS cells. The maintenance of the undifferentiated stage of pluripotent stem cells was further evaluated by the detection of pluripotency-related biomarkers such as Oct3/4 or SSEA-1. Mouse ES cell colonies maintained a dome-like appearance and retained the expression of Oct3/4 and SSEA-1 molecules when the cells were cultured with 2×10^5 cubes of H1/LIF polyhedra or 10 ng/mL of rhLIF, but not with LIF/VP3 polyhedra or with CP-H polyhedra (Fig. 4A and B). An epithelium-like colony emerged and loss of SSEA-1 or Oct3/4 expression was observed when the cells were cultured in the absence of rhLIF (data not shown), as was observed in cell cultures with CP-H or LIF/VP3 polyhedra.

Like the mouse ES cell colonies, mouse Oct-4-GFP knock-in iPS cell colonies (iWF-1) cultured with rhLIF and H1/LIF maintained a dome-shape morphology, SSEA-1 expression at a molecular level, and Oct3/4 at a transcriptional level, but such cultures in the presence of LIF/VP3 or CP-H polyhedra did not (Fig. 4C and D), analogous to the results shown in Fig. 3. Morphology of the iPS cell colonies cultured with LIF/VP3 polyhedra was distinct from that with H1/LIF polyhedra. Dish-like colonies emerged when cultured with LIF/VP3, but the rim of these colonies were detached from the gelatin-coated dish and formed embryoid body-like cell clumps. These cell clusters did not express SSEA-1 at the center of the colony. Interestingly, EB5 cells spontaneously start to differentiate as an adhesive cell, while iWF-1 cells lose adhesive properties and start to differentiate following LIF depletion. It is presumed that difference in epigenetic status may account for a distinct cellular behavior in differentiation upon LIF depletion in these two cell lines. The exact mechanism shall be elucidated in future study.

3.4. Addition of H1/LIF polyhedra sustains ES cell growth in a dose-dependent manner

The effect of LIF polyhedra on mouse ES iPS cell proliferation during short-term (7-day) culture was determined by assessing cell number at days 3 and 5. Of particular note, the proliferation potential afforded by 2×10^5 cubes of H1/LIF polyhedra is equivalent to that of 10 ng/mL rhLIF and far superior to that of LIF/VP3 (Fig. 5A and C). In addition, ES cells proliferated in a dose-dependent manner within the range of 7.5×10^3 to 2×10^5 cubes of H1/LIF polyhedra (Fig. 5B).

The slow release effect of H1/LIF polyhedra was determined by assessing cell number during ES cell culture over 2 weeks. ES cells were cultured either with 2×10^5 cubes or 5×10^5 cubes of H1/LIF polyhedra or 10 ng/mL rhLIF, and cell numbers were determined at days 3, 5, 7, and 14. The rhLIF was added to the culture media at days 0, 3, 5, 7, 10 and 12 to sustain cell proliferation, while H1/LIF polyhedra were added just once, at the start of the culture. H1/LIF
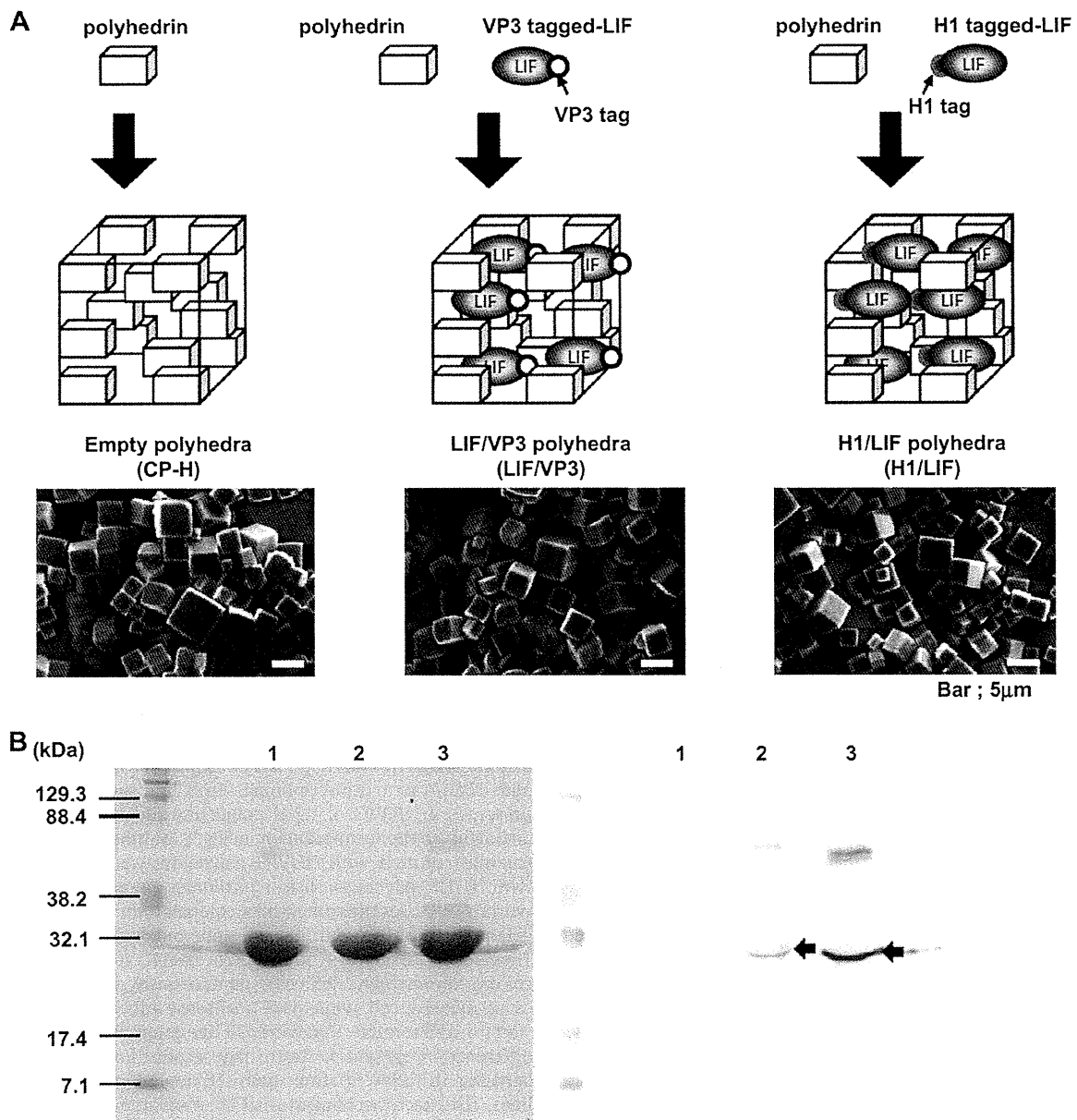
Fig. 1. (A) Schema for the generation of LIF slow-releasing agents (LIF-containing polyhedra), and corresponding photos of polyhedra crystals. Either H1-tagged LIF or VP3-tagged LIF was immobilized into polyhedra to generate two types of slow-releasing agents, namely H1/LIF polyhedra (H1/LIF) or LIF/VP3 polyhedra (LIF/VP3). Empty polyhedra (CP-H) consisting solely of BmCPV polyhedrin protein were used as a control. (B) Detection of LIF immobilized into polyhedra by SDS-PAGE and western blotting. LIF immobilized into polyhedra was analyzed by electrophoresis on 12.5% polyacrylamide gels (left panel) and detected by western blotting (right panel) with an anti-LIF monoclonal antibody. Lanes 1, 2, and 3 correspond to CP-H, LIF/VP3, and H1/LIF samples, respectively. Arrows show the bands corresponding to human LIF molecule.

polyhedra showed a slow-releasing effect, as 5×10^5 cubes of H1/LIF polyhedra sustained ES cell proliferation at a comparable level to that seen with the cell culture where 10 ng/mL rhLIF is added every 2–3 days (Fig. 5D).

3.5. Signaling delivered by H1/LIF polyhedra is persistent

Propagation of LIF-stimulated intracellular signaling is mediated by STAT3 activation [20], which can be determined by the detection of phosphorylated STAT3. Indeed, addition of rhLIF or H1/LIF polyhedra to a rhLIF-starved EB5 cell culture induced a spike in STAT3 phosphorylation at 3 and 6 h (Fig. 6). The STAT3 phosphorylation induced by rhLIF rapidly falls to basal levels by day 3 at the single cell level, and additional 10 ng/mL rhLIF is needed to resume increased STAT3 phosphorylation levels. STAT3 phosphorylation was also assayed 6 h after the addition of rhLIF on days 3 and 5. A similar induction of STAT3 phosphorylation was observed 6 h after adding rhLIF on days 3 and 5 of the culture followed by reduction of STAT3 phosphorylation at days 5 and 7. However, the magnitude of the phospho-STAT3 induction is attenuated over the course of the culture at the single cell level due to an increased total cell number (Fig. 6). In contrast, when 2×10^5 cubes of H1/LIF polyhedra were
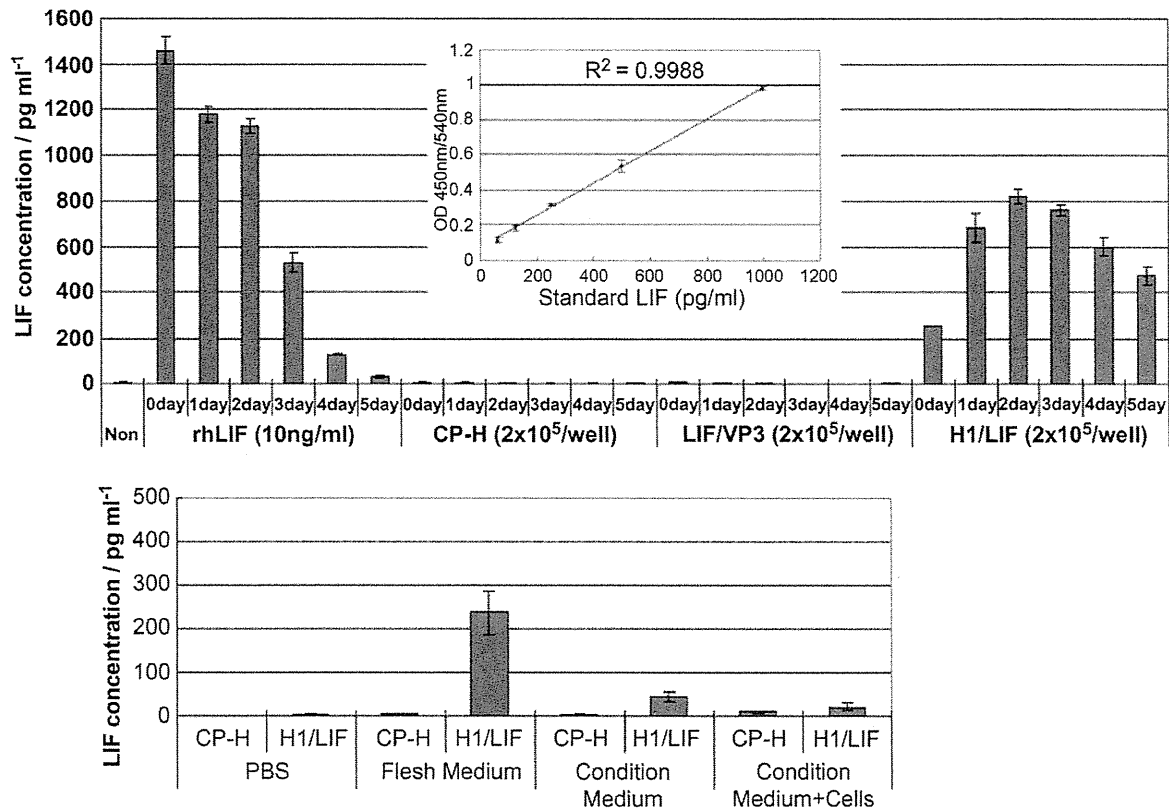
Fig. 2. Concentration of human LIF in ES cell culture media from designated culture conditions. ES cells were cultured either with 10 ng/mL rhLIF, or with 2×10^5 each of cubes of empty CP-H polyhedral (CP-H), LIF/VP3 polyhedra (LIF/VP3), or H1/LIF polyhedra (H1/LIF) (Upper panel). The amount of LIF in culture media from an individual sample was determined by ELISA and the measured value is shown as a bar, with an error bar indicating standard deviation (X-axis, different treatments and times; Y-axis, amount in pg/ml). Samples taken 1 h after the culture was initiated were designated as being collected at day 0. In addition, the amount of human LIF released from 2×10^5 cubes of CP-H or H1/LIF polyhedra that were suspended for 1 h in PBS, fresh media for EB5 (Fresh Medium), conditioned media from 3-day-old EB5 culture (Condition Medium), or 3-day-old EB5 cell culture (Condition Medium + Cells) was also determined (Lower panel). The inset shows the calibration curve and the best-fit lines used for converting optical density (OD) to concentration values.

added to EB5 cells at the start of the culture, the sharp activation of STAT3 decreases slowly over time, as determined by measurements made at day 3 + 6 h, day 5 + 6 h, and day 7 + 6 h. The concentration of LIF in culture media under various culture conditions shown in Fig. 2 also supported these results.

4. Discussion

Our study demonstrates that H1/LIF polyhedra, which immobilized human LIF into polyhedra via the H1-tag, possess long-acting biological activities in ES cell culture, with effects comparable to
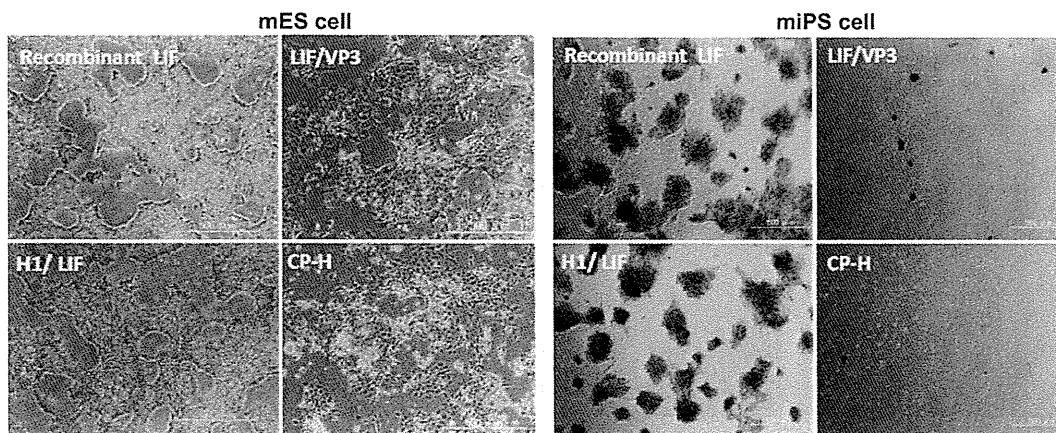

Fig. 3. Biological effect of H1/LF and LIF/VP3 on the maintenance of ES cells. Mouse ES cells (EB5 cells; left panels) or mouse iPS cells (iWF-1 cells; right panels) were cultured with 10 ng/mL rhLIF (upper left) or with 2×10^5 cubes of LIF/VP3 (upper right), H1/LIF (lower left) or CP-H (lower right) polyhedra for 5 days, followed by ALP staining.
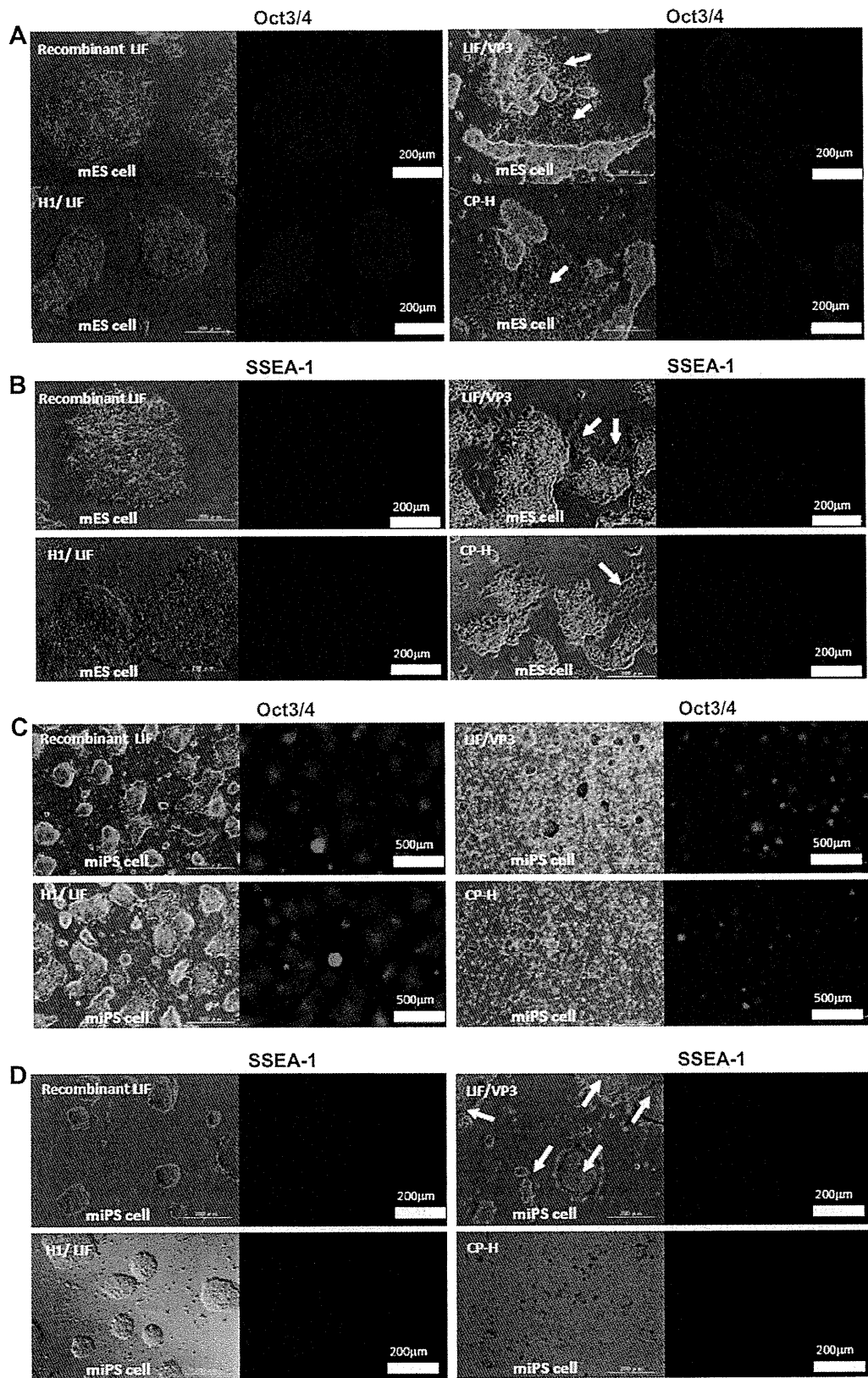
Fig. 4. Expression of pluripotency-related markers in ES cells cultured with polyhedra. Expression of Oct3/4 (A), SSEA-1 (B) in cultured EB5 cells, or Oct3/4 (C), SSEA-1 (D) in cultured mouse iPS cells (iWF-1 cells) with 10 ng/mL rhLIF (upper left) or 2 × 10⁵ cubes of LIF/VP3 (upper right), H1/LIF (lower left) or CP-H (lower right) polyhedra are shown. Cells were cultured with respective agents for 5 days and fixed for immunostaining. A phase-contrast image (left) and the corresponding immunostaining image (right) under a fluorescent microscope are shown.
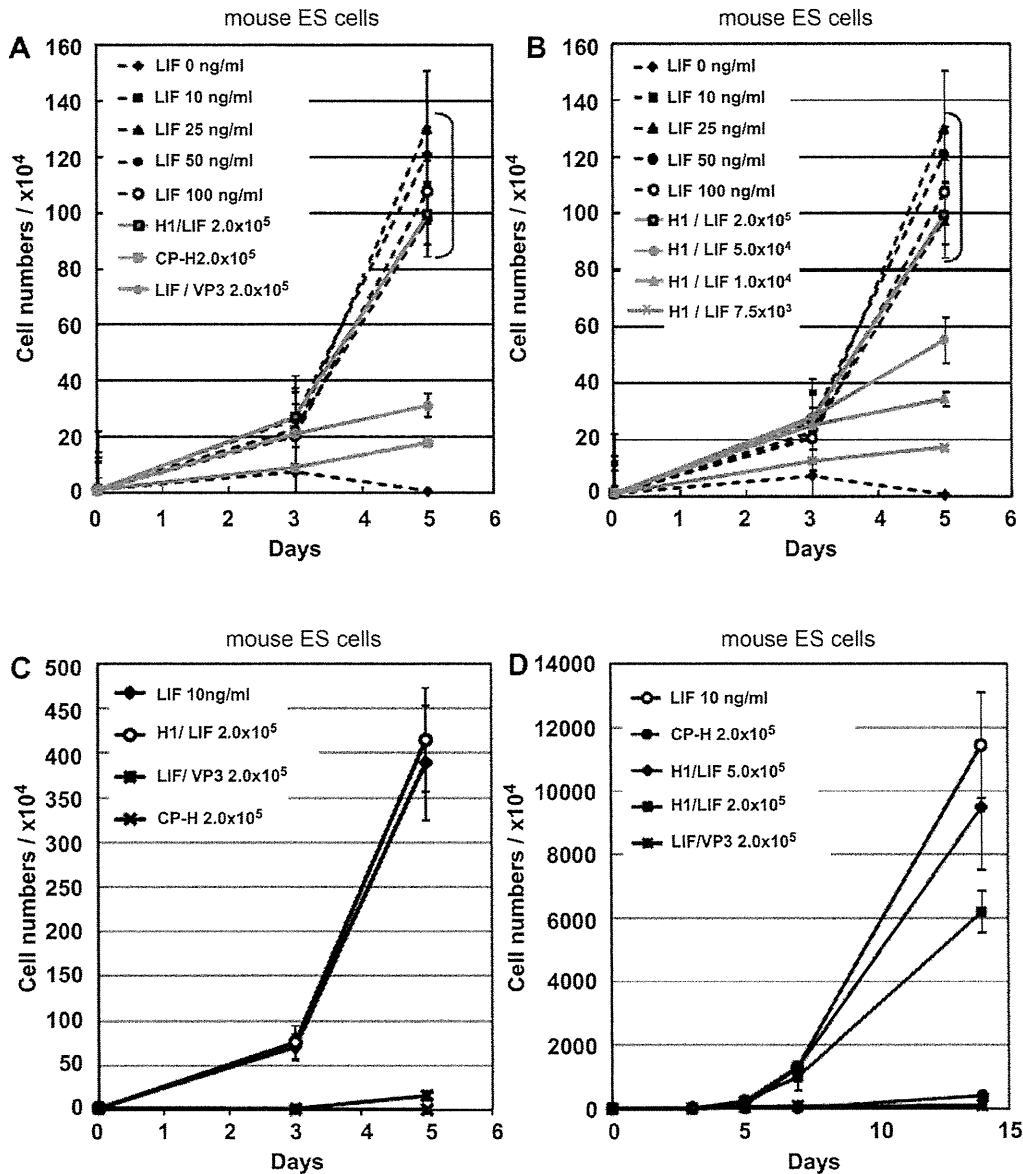
Fig. 5. Addition of H1/LIF promotes the growth of pluripotent stem cells in a dose-dependent manner. Results are shown as linear graphs with mean and standard deviation (SD; indicated by error bars) derived from 3 independent experiments. A: mouse ES cells proliferate in the presence of H1/LIF polyhedra. Either 2×10^5 cubes of H1/LIF, LIF/VP3, or CP-H polyhedra were added to 1×10^4 EB5 cells at the beginning of the culture, while 10, 25, 50 or 100 ng/mL rhLIF was added at days 0 and 3 of the culture to sustain cell proliferation. The number of cells was assessed at days 3 and 5. B: ES cells proliferate by the addition of H1/LIF polyhedra in a dose-dependent manner. Either 7.5×10^3, 1.0×10^4, 5.0×10^4 or 2.0×10^5 cubes of H1/LIF polyhedra were added to 1×10^4 EB5 cells at the beginning of the culture, while 10, 25, 50 or 100 ng/mL rhLIF was added at days 0 and 3 of the culture to sustain cell proliferation. The number of cells was assessed at days 3 and 5. C: Mouse iPS cells proliferate in the presence of H1/LIF polyhedra. Either 2×10^5 cubes of H1/LIF, LIF/VP3, or CP-H polyhedra were added to 1×10^4 EB5 cells at the beginning of the culture, and 10 ng/mL rhLIF was added at days 0 and 3 to sustain cell proliferation. The number of cells was assessed at days 3 and 5. D: H1/LIF polyhedra sustain the proliferation of mouse ES cells for 2 weeks. Ten thousand EB5 cells were cultured with either 10 ng/mL rhLIF, 2×10^5 cubes or 5×10^5 cubes of H1/LIF polyhedra, 2×10^5 cubes of LIF/VP3 polyhedra, or 2×10^5 cubes of CP-H polyhedra for 14 days. The number of cells was assessed at days 3, 5, 7, and 14. rhLIF was added at days 0, 3, 5, 7, 10 and 12, while polyhedra were only added at the start of corresponding cultures.

those seen for a periodic administration of rhLIF protein to the culture media. The mechanism underlying how LIF is released from H1/LIF polyhedra but not from LIF/VP3 polyhedra remains elusive, and further protein crystal analysis is needed to provide full answers. Nonetheless, our findings suggest that inexpensive H1/LIF polyhedra can be productively used to sustain a long-term and a closed mass culture system.

Recently, a biocarrier using immobilized LIF on a maleic anhydride copolymer thin-film was reported [21]. Here, the immobilized LIF protein regulated the pluripotency of ES cells growing on the film

for 2 weeks. The ES cell colony spread radially and notably the cells in the center of the colony, not at the rim of the colony, could use up LIF immobilized in the film, resulting in differentiation from the center of colony due to deficient LIF stimulation. In this report, we demonstrate the biological potential of immobilizing LIF into polyhedra (e.g. H1/LIF), which can then be mixed with the culture medium as a soluble, slow-releasing agent of LIF, thereby obviating the need to add rhLIF to the culture medium every 2–3 days to maintain ES cell proliferation. Furthermore, unlike rhLIF that induces spikes in STAT3 phosphorylation (Fig. 6) and cellular
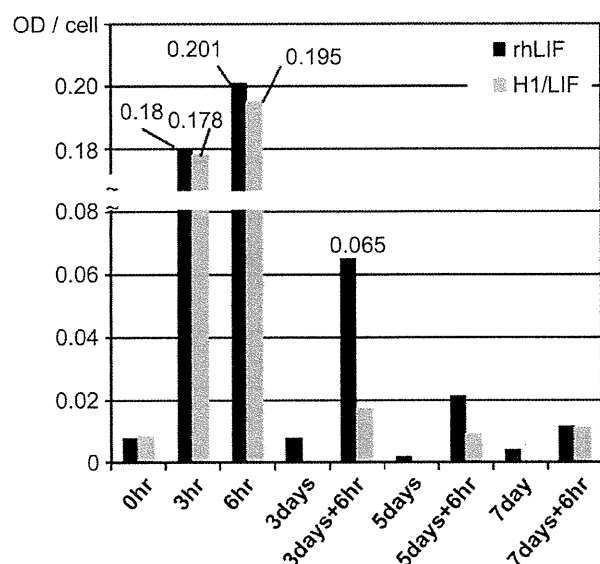
Fig. 6. STAT3 activation at a single cell level. Ten thousand EB5 cells were cultured either with 10 ng/mL rhLIF (black bar) or 2 × 10^5 cubes of H1/LIF polyhedra (gray bar). The activated form of STAT3 (phosphorylated STAT3), measured in OD units at designated time points at a single cell level, is shown.

response [13], use of the slow-releasing agent H1/LIF provided a persistent STAT3-mediated signal activation through continuous LIF release into the culture medium. This slow-releasing property, we presume, will be beneficial for the maintenance and proliferation of ES cells by avoiding the fluctuations (or disruptions) in intracellular signaling through periodic ligand stimulation and starvation.

Recently, two distinct pluripotency stages of the mouse ES cell, namely the inner cell mass (ICM)-type stem cell and Epiblast-type stem cells (EpiSCs) have been reported [22–27]. ICM-type mouse ES cells are "bona fide" pluripotent stem cells representing the pre-implantation blastocysts that are able to contribute to chimerism when placed back into blastocysts, and require LIF for the maintenance and proliferation of ES cells. While EpiSCs ES cells, which represent the post-implantation stage epiblasts, demonstrate the potential to differentiate into three germ lines *in vitro*, these cells are incapable of contributing to chimerism. EpiSCs require basic fibroblast growth factor (bFGF) for the maintenance and proliferation of ES cells. Both human ES cells and human iPS cells seem to correspond to the EpiSCs with respect to colony morphology, gene expression profiles, and cytokine requirement [25], but can be converted to the ICM-type stem cell stage by cultivation [28] or by constitutive activation of *Klf2/Klf4* genes [26,27] in the presence of LIF. These reports suggest the potential applications of H1/LIF polyhedra for the maintenance of ICM-type human ES cells and human iPS cells in a closed culture system in future study. In the course of reviewing process of this paper we have succeeded to culture human naïve iPS cells with H1/LIF and show the result in Supplementary figure.

5. Conclusions

Human LIF was immobilized into insect virus polyhedra (LIF polyhedra) and release of LIF protein from LIF polyhedra was observed for at least 5 days. Mouse ES cells and mouse iPS cells were proliferated by adding LIF polyhedra in a dose-dependent manner. Both ES cells and iPS cells formed colonies and were stained by Alkali phosphatase positively. Expression of Oct3/4 and SSEA-1 of ES and iPS colony was also determined. A single addition

of LIF polyhedra to the ES cell culture medium supported the proliferation of both ES cells continuously for 14 days.

Acknowledgment

Appendix

Figures with essential colour discrimination. Figs. 1, 5 and 6 in this article are difficult to interpret in black and white. The full colour images can be found in the online version, at doi:10.1016/j.biomaterials.2010.12.063.

Appendix. Supplementary material

Supplementary data related to this article can be found online at doi:10.1016/j.biomaterials.2010.12.063.

References

[1] Smith AG, Nichols J, Robertson M, Rathjen PD. Differentiation inhibiting activity (DIA/LIF) and mouse development. Dev Biol 1992;151(2):339–51.
[2] Moreau JF, Donaldson DD, Bennett F, Witek-Giannotti J, Clark SC, Wong GG. Leukaemia inhibitory factor is identical to the myeloid growth factor human interleukin for DA cells. Nature 1988;336(6200):690–2.
[3] Niwa H, Miyazaki J, Smith AG. Quantitative expression of Oct-3/4 defines differentiation, dedifferentiation or self-renewal of ES cells. Nat Genet 2000;24(4):372–6.
[4] Hirata H, Kawamata S, Murakami Y, Inoue K, Nagahashi A, Tosaka M, et al. Coexpression of platelet-derived growth factor receptor alpha and fetal liver kinase 1 enhances cardiogenic potential in embryonic stem cell differentiation in vitro. J Biosci Bioeng 2007;103(5):412–9.
[5] Hirano T, Nakajima K, Hibi M. Signaling mechanisms through gp130: a model of the cytokine system. Cytokine Growth Factor Rev 1997;8(4):241–52.
[6] O'Shea JJ, Gadina M, Schreiber RD. Cytokine signaling in 2002: new surprises in the Jak/Stat pathway. Cell 2002;109(2):S121–31.
[7] Darnell Jr JE. STATs and gene regulation. Science 1997;277(5332):1630–5.
[8] Lutticken C, Wegenka UM, Yuan J, Buschmann J, Schindler C, Ziemiecki A, et al. Association of transcription factor APRF and protein kinase Jak1 with the interleukin-6 signal transducer gp130. Science 1994;263(5143):89–92.
[9] Niwa H, Burdon T, Chambers I, Smith A. Self-renewal of pluripotent embryonic stem cells is mediated via activation of STAT3. Genes Dev 1998;12(13):2048–60.
[10] Boeuf H, Hauss C, Graeve FD, Baran N, Kedinger C. Leukemia inhibitory factor-dependent transcriptional activation in embryonic stem cells. J Cell Biol 1997;138(6):1207–17.
[11] Owczarek CM, Zhang Y, Layton MJ, Metcalf D, Roberts B, Nicola NA. The unusual species cross-reactivity of the leukemia inhibitory factor receptor alpha-chain is determined primarily by the immunoglobulin-like domain. J Biol Chem 1997;272(38):23976–85.
[12] Huyton T, Zhang JG, Luo CS, Lou MZ, Hilton DJ, Nicola NA, et al. An unusual cytokine: Ig-domain interaction revealed in the crystal structure of leukemia inhibitory factor (LIF) in complex with the LIF receptor. Proc Natl Acad Sci U S A 2007;104(31):12737–42.
[13] Davey RE, Onishi K, Mahdavi A, Zandstra PW. LIF-mediated control of embryonic stem cell self-renewal emerges due to an autoregulatory loop. FASEB J 2007;21(9):2020–32.
[14] Belloncik S, Mori H. Cypoviruses. In: Miller LK, Ball LA, editors. The insect viruses. New York Plenum Press; 1998. p. 337–69.
[15] Coulibaly F, Chiu E, Ikeda K, Gutmann S, Haebel PW, Schulze-Briese C, et al. The molecular organization of cypovirus polyhedra. Nature 2007;446(7131):97–101.
[16] Ikeda K, Nakazawa H, Shimo-Oka A, Ishio K, Miyata S, Hosokawa Y, et al. Immobilization of diverse foreign proteins in viral polyhedra and potential application for protein microarrays. Proteomics 2006;6(1):54–66.
[17] Yoshimizu T, Sugiyama N, De Felice M, Yeom YI, Ohbo K, Masuko K, et al. Germline-specific expression of the Oct-4/green fluorescent protein (GFP) transgene in mice. Dev Growth Differ 1999;41(6):675–84.
[18] Takahashi K, Yamanaka S. Induction of pluripotent stem cells from mouse embryonic and adult fibroblast cultures by defined factors. Cell 2006; 126(4):663–76.
[19] Ijiri H, Coulibaly F, Nishimura G, Nakai D, Chiu E, Takenaka C, et al. Structure-based targeting of bioactive proteins into cypovirus polyhedra and application to immobilized cytokines for mammalian cell culture. Biomaterials 2009; 30(26):4297–308.